L. Li, H.R. Maier, M.F. Lambert, C.T. Simmons, D. Partington

Framework for assessing and improving the performance of recursive digital filters for baseflow estimation with application to the Lyne and Hollick filter

Environmental Modelling & Software, 2013; 41:163-175

Framework for assessing and improving the performance of recursive digital filters for baseflow estimation with application to the Lyne and Hollick filter

by

Li, L., Maier, H.R., Lambert, M.F., Simmons, C.T., Partington, D.

Environmental Modelling and Software

Elsevier Editorial System(tm) for Environmental Modelling & Software
Manuscript Draft

Manuscript Number: ENVSOFT-D-12-00402R1

Title: Framework for Assessing and Improving the Performance of Recursive Digital Filters for Baseflow Estimation with Application to the Lyne and Hollick Filter

Article Type: Research Paper

Keywords: baseflow estimation; fully integrated surface water/ground water model; digital filters, framework

Corresponding Author: Ms Li Li, B.E., M.E.

Corresponding Author's Institution: School of Civil, Environmental & Mining Engineering

First Author: Li Li, MEngSc

Order of Authors: Li Li, MEngSc; Holger R Maier, Professor; Martin F Lambert, Professor; Craig T Simmons, Professor; Daniel Partington, BE

Abstract: Baseflow is often regarded as the streamflow component derived predominantly from groundwater discharge. The estimation of baseflow is important for water supply, water allocation, investigation of contamination impacts, low flow hydrology and flood hydrology. Baseflow is commonly estimated using graphical methods, recursive digital filters (RDFs), tracer based methods, and conceptual models. Of all of these methods, RDFs are the most commonly used, due to their relatively easy and efficient implementation. This paper presents a generic framework for assessing and improving the performance of RDFs for baseflow estimation for catchments with different characteristics and subject to different hydrological conditions. As part of the framework, a fully integrated surface water/groundwater (SW/GW) model is used to obtain estimates of streamflow and baseflow for catchments with different properties, such as soil types and rainfall patterns. A RDF is then applied to the simulated streamflow to assess how well the baseflow obtained using the filter matches the baseflow obtained using the fully integrated SW/GW model. In order to improve the performance of the filter, the user-defined parameter(s) controlling filter operation can be adjusted in order to obtain the best match between the baseflow obtained using the filter and that obtained using the fully integrated SW/GW model (i.e. through calibration). The proposed framework is tested by applying it to a common SW/GW benchmarking problem, the tilted V-catchment, for a range of soil properties. HydroGeoSphere (HGS) is used to develop the fully integrated SW/GW model and the Lyne and Hollick (LH) filter is used as the RDF. The performance of the LH filter is assessed using the commonly used value of the filter parameter of 0.925, as well as calibrated filter parameter values. The results obtained show that the performance of the LH filter is affected significantly by the saturated hydraulic conductivity (Ks) of the soil and that calibrated LH filter parameter can result in significant improvements in filter performance.

Response to Reviewers: Please refer to the attached 'Response to Reviewers' document.

RESPONSE TO REVIEWERS' COMMENTS

Manuscript Reference code: ENVSOFT-D-12-00402

Title: Framework for Assessing and Improving the Performance of Recursive Digital Filters for Baseflow Estimation with Application to the Lyne and Hollick Filter

Corresponding Author: Li Li (The University of Adelaide)

Contributing Authors: Maier H.R., Lambert M.F., Simmons C.T., Partington D.

Line numbers refer to line numbers generated in word document—Manuscript with line numbers, NOT the numbers in the PDF file. A copy of this word document can be found in Supplementary Material.

Reviewer #1 comments:

1.1 *I have reviewed a previous version and the manuscript has improved considerably. Neverless, I think the authors should give it a very carefully re-read as there is still significant potential to improve the paper. See below for details. Some aspects of the paper remain unclear, e.g. Figures 8 and 12 are incomprehensible and the way the linear uncertainties are obtained is not clear as the parameters in the equations are not explained. The role of the uncertainty analysis as such is also unclear and there is no mention of it in the conclusions.*

Response: Figures 8 and 12, as well as the uncertainty analysis, were added in response to the comments by another reviewer, who is now happy with the revisions (reviewer 2 below). Consequently, the authors do not think they should be changed or removed. The authors believe that Figures 8 and 12 provide valuable insight/explanation and are not considered incomprehensible, as they are standard flow duration curves, which have been used extensively in surface hydrology since about 1880 (Vogel and Fennessey, 1994). However, in order to provide a brief explanation of what flow duration curves are and why they were used, the material related to Figure 8 has been moved to a separate paragraph as follows (starting at line 411):

> "This difference in the streamflow behavior for the two different soil types can also be seen clearly by examining the corresponding flow duration curves, which are an estimate of the percentage of time a particular streamflow was equaled or exceeded, and therefore provide a graphical representation of the variability associated with streamflow (Vogel and Fennessey, 1994). As can be seen from Fig. 8, the flow duration curve for the catchment with a sandy soil is very flat, indicating that streamflow is almost constant over time, which is representative of a stream that is fed primarily by baseflow. In contrast, the flow duration curve for the catchment consisting of silt loam indicates that flows are highly variable, with higher peak flows, but extended periods with little or no flow, which is indicative of a catchment that is dominated by surface flow."

In relation to the use of "uncertainty analysis", the purpose of obtaining bounds on the parameter estimates was to determine whether the optimal filter parameter values are well defined or not, which provides an indication of the degree of confidence that can be placed in the results, such as the relationship between K_s and optimal filter parameter values. This has been clarified in the revised version of the manuscript as shown below (starting at lines 378 and 432). This is not an uncertainty analysis of the results, but considered good practice in model calibration. As such, this information is not included in the conclusions.

> "As can be seen, the uncertainty estimates are very small, indicating that the optimal values of the filter parameters are well defined and that the results obtained can be treated with confidence."

> "The results obtained for all of the simulations conducted are shown in Fig. 10, including the linear estimates of uncertainty, which are very small, indicating that the results obtained can be treated with confidence."

Vogel, R.M., Fennessey, N.M., 1994. Flow-duration curves. I: New interpretation and confidence intervals. Journal of Water Resources Planning and Management 120(4) 485-504.

1.2 *Reformulation of some paragraphs as well as removing repetitions would make the paper easier to read.*

Response: A thorough editorial review of the paper has been conducted of the paper and changes have been made to the paper to address this issue where deemed appropriate, as shown in the "track changes" version of the revised manuscript. In the absence of more specific guidance by the reviewer, that is all that could be done.

1.3 *I also suggest reducing the number of figures, e.g. are figures 8 and 12 really required?*

Response: As per the response to Comment 1.1, the figures were added in response to comments of another reviewer and do provide valuable insight.

1.4 *The paper is very long to make the points listed in the conclusions (basically the second paragraph)*

Response: The authors do not believe that the paper is very long. Part of the paper introduces the generic framework, which is also a contribution of the paper, not just the results of the analysis.

Detailed comments:

1.5 *Page 5 Last sentence: remove that recommendations are given in the conclusion section (or add some recommendation to the conclusions).*

Response: This sentence has been edited and now reads (starting from line 123):

“The results obtained for the case study are presented and discussed in Section 4 and a summary and conclusions are given in Section 5.”

<u>1.6</u> *Page 8 line 58: delete “so as”.*

<u>Response</u>: The authors have assumed that the “so as” being referred to in this comment is actually in line 34/35 of page 8, and we have amended it to read (starting from line 173):

> “Based on the assumption that the simulated baseflow obtained using the fully integrated SW/GW model (q_b^{sim}) is representative of the ‘real’ baseflow, the filter parameter(s) (θ) can be adjusted to minimize an error measure between the ‘real’ baseflow (q_b^{sim}) and the baseflow computed using the RDF (q_b^{filter}).”

<u>1.7</u> *Page 6, paragraph following the title “performance assessment”: This can be shortened. The aspects related to St. Venant and Richards equations do not help to make the point made in line 38-42.*

<u>Response</u>: This paragraph has been edited and now reads (starting from line 140):

> “The proposed framework for assessing the performance of RDFs under a range of physical catchment conditions is shown in Fig. 1. As mentioned above, the underlying premise of the proposed approach is that a fully integrated SW/GW model provides the best possible approximation to the physical processes of water flow within catchments and can therefore be used as an approximation to such processes subject to a variety of physical characteristics and forcings. This is because rainfall is allowed to partition into overland flow, streamflow, evaporation, infiltration and recharge in a physically based fashion (Therrien et al., 2009), without prior definition of flow generation processes or storage discharge relationships. All of the governing flow equations implemented by the fully integrated SW/GW model are solved simultaneously to obtain the simulated streamflow (q) and baseflow (q_b^{sim}) as a function of user-defined catchment characteristics (e.g. soil types, catchment size, catchment shapes) and hydrological inputs (e.g. rainfall patterns, antecedent moisture, evaporation) (Fig. 1).”

<u>1.8</u> *Table 1: It is the authors call, but some of the values listed (especially porosity for clay) are out of range, no matter what is mentioned in the cited Puhlman paper. The numbers in the paper by Puhlman are (as the title suggests) model results from forest soils, not measured values. Also note that, contrary to the statement in the reviewers response, Carsel and Parrish do provide a mean and a standard variation and base their values on a large number of measurements, not on fitted models. The paper can proceed without repeating the simulations, but for further considerations I suggest to read the Carsel and Parrish paper.*

<u>Response</u>: The reviewer is correct in stating the values of the soil parameters given in Puhlmann are model results from forest soils, and porosity for clay is especially out of range, compared with the measured values in Carsel and Parrish. However, as mentioned in the previous response to reviewers, almost all of the soil parameters used in the Carsel and Parrish paper are included in the ranges of the values given by Puhlman. Furthermore, clay was not considered in this paper.

1.9 *Page 12, paragraph on HGS: Carefully re-read, the logic breaks down from the second and third sentence.*

Response: The reviewer is correct that the second sentence breaks down the logic between the first and the third sentence. Therefore, the second sentence was removed from this paragraph and now reads (starting from line 252):

> "All of the equations above are solved simultaneously at each time step utilising either a finite difference, control volume finite difference or finite element approach (Therrien et al., 2009). For this study, the control volume finite difference method is used, due to its quick implementation on regular model grids and superior mass conservation (Partington et al., 2009)."

1.10 *The description of the model is a bit repetitive (e.g. page 14, line 23-25 was said in the first paragraph and somewhere in the introduction).*

Response: The information provided is brief and of a general nature, whereas the information provided on page 14 is more comprehensive and specific to the LH filter. Consequently, the authors believe that the repetition of information contained in ~1.5 lines is warranted and adds to ease of understanding of the material in the paper.

1.11 *In the text (P14), it is mentioned that the vertical resolution is 0.5m, in the response 0.05. The figure suggests that 0.05 was used. This would be an appropriate resolution.*

Response: The reviewer was correct in pointing out that the vertical resolution depicted in the text (0.5m) is different from the response to reviewers (0.05m), which was described incorrectly and has been corrected in the current version, that the vertical discretization used for the model simulation should be 0.5m. The improved vertical discretization of 0.5m used is based on previous studies using the V-catchment as a basis (e.g. Partington et al., 2011; Partington et al., 2012).

Partington, D., Brunner, P., Simmons, C.T., Therrien, R., Werner, A.D., Dandy, G.C., Maier, H.R., 2011. A hydraulic mixing-cell method to quantify the groundwater component of streamflow within spatially distributed fully integrated surface water-groundwater flow models. Environmental Modelling & Software 26(7) 886-898.

Partington, D., Brunner, P., Simmons, C.T., Werner, A.D., Therrien, R., Maier, H.R., Dandy, G.C., 2012. Evaluation of outputs from automated baseflow separation methods against simulated baseflow from a physically based, surface water-groundwater flow model. Journal of Hydrology 458-459 28-39.

1.12 *Uncertainty associated with LH filter parameters: This is in the chapter on error measure and optimization procedure, but the optimization procedure is not really described here. How was the objective function minimized?*

Response: The objective function used for optimisation procedure is the Nash-Sutcliffe coefficient of efficiency (E_f), and the Golden Section Search Method was the optimisation method used to determine the optimal filter parameter (i.e. the filter parameter that results in the maximum E_f value), as discussed in Section 3.4. In order to clarify this, a reference to the Golden Section Search Method has been added and the sentence explaining how the parameter optimisation procedure was conducted has been clarified as follows (starting at line 373):

> "The optimisation method used in order to obtain the optimal values of the filter parameters was the golden section search method (Press et al. 1992), as there was only one model parameter."

The procedure for calibrating the filter parameters was described as part of the generic model improvement framework in Section 2.2 (see excerpt below, starting from line 172) and was not re-stated in Section 3.4 in order to avoid repetition.

> "In order to determine the best possible values of the filter parameters for a given catchment, the assessment framework introduced in the previous section can be extended, as shown in Fig. 2. Based on the assumption that the simulated baseflow obtained using the fully integrated SW/GW model (q_b^{sim}) is representative of the 'real' baseflow, the filter parameter(s) (θ) can be adjusted to minimize an error measure between the 'real' baseflow (q_b^{sim}) and the baseflow computed using the RDF (q_b^{filter}).Any of the performance measures mentioned in Section 2.1 can be used for this purpose. Alternatively, a multi-objective approach can be adopted (e.g. Gibbs et al., 2012). This calibration process can be automated using various optimization methods, such as gradient based methods or evolutionary algorithms, depending on the complexity of the calibration problem (e.g. the number of parameters to be estimated)."

1.13 *Also, I just could not follow the equations. What is qbsilter?*

Response: The expression qbsilter was incorrect in the previous version of the manuscript, and has been corrected in the revised version and shown below:

$$S(k) = \sum_{i=1}^{n} [q_{b(i)}^{filter}(k) - q_{b(i)}^{sim}]^2 \qquad (11)$$

1.14 *Shouldn't the index be k, not n?*

Response: The index in the equations (10) and (11) should be *k*. As per response to Comment 1.13, Equation (11) has been modified to show a clearer expression of *S(k)*, which is the sum of squared error between the baseflow obtained using the LH filter and that simulated using the HGS model at each time step *i*. Also, it can be seen from equation (11) that *S(k)* is a function of the filter parameter *k*, not *n*.

1.15 *The values on lower bound and upper bound are basically identical (table 2), I am not sure if this adds a lot to the paper.*

<u>Response:</u> The reviewer is correct that the values on the lower and upper bound are basically identical. However, the uncertainty analysis was added in response to the comment of another reviewer. Also, the authors respectfully disagree that this does not add anything, as it shows that there is very little uncertainty associated with the estimates, which provides additional confidence in the findings. This has now been made clearer in the paper (starting at lines 378 and 432).

> "As can be seen, the uncertainty estimates are very small, indicating that the optimal values of the filter parameters are well defined and that the results obtained can be treated with confidence."

> "The results obtained for all of the simulations conducted are shown in Fig. 10, including the linear estimates of uncertainty, which are very small, indicating that the results obtained can be treated with confidence."

<u>1.16</u> *In any case the description of the equations has to be fixed.*

<u>Response:</u> Given that equations (10) and (11) are standard, well known equations and that an appropriate reference is provided, the authors believe that fixing the terminology/ symbols is all that is required.

<u>1.17</u> *All figure captions are still in ML, contrary to the response to the reviewers.*
and
<u>1.18</u> *Some labels of figure axes are cut off. I still think the labelling of the figures can be improved.*

<u>Response to Comments 1.17 & 1.18:</u> All of the figures with ML units, cut off axes and unclear labelling have been redrawn and are shown below:

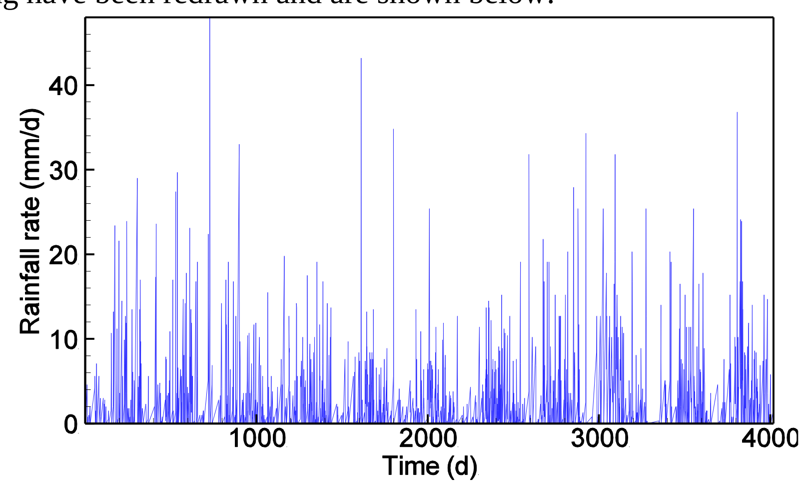

Fig. 4 10 year daily rainfall data for Adelaide, South Australia, gauge number 23000

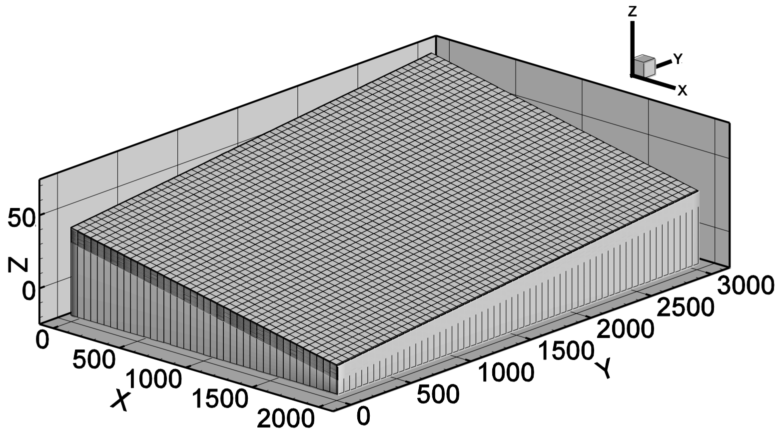

Fig. 5 Catchment model for case study (modified version of the V-catchment in Pandy and Huyakorn (2004))

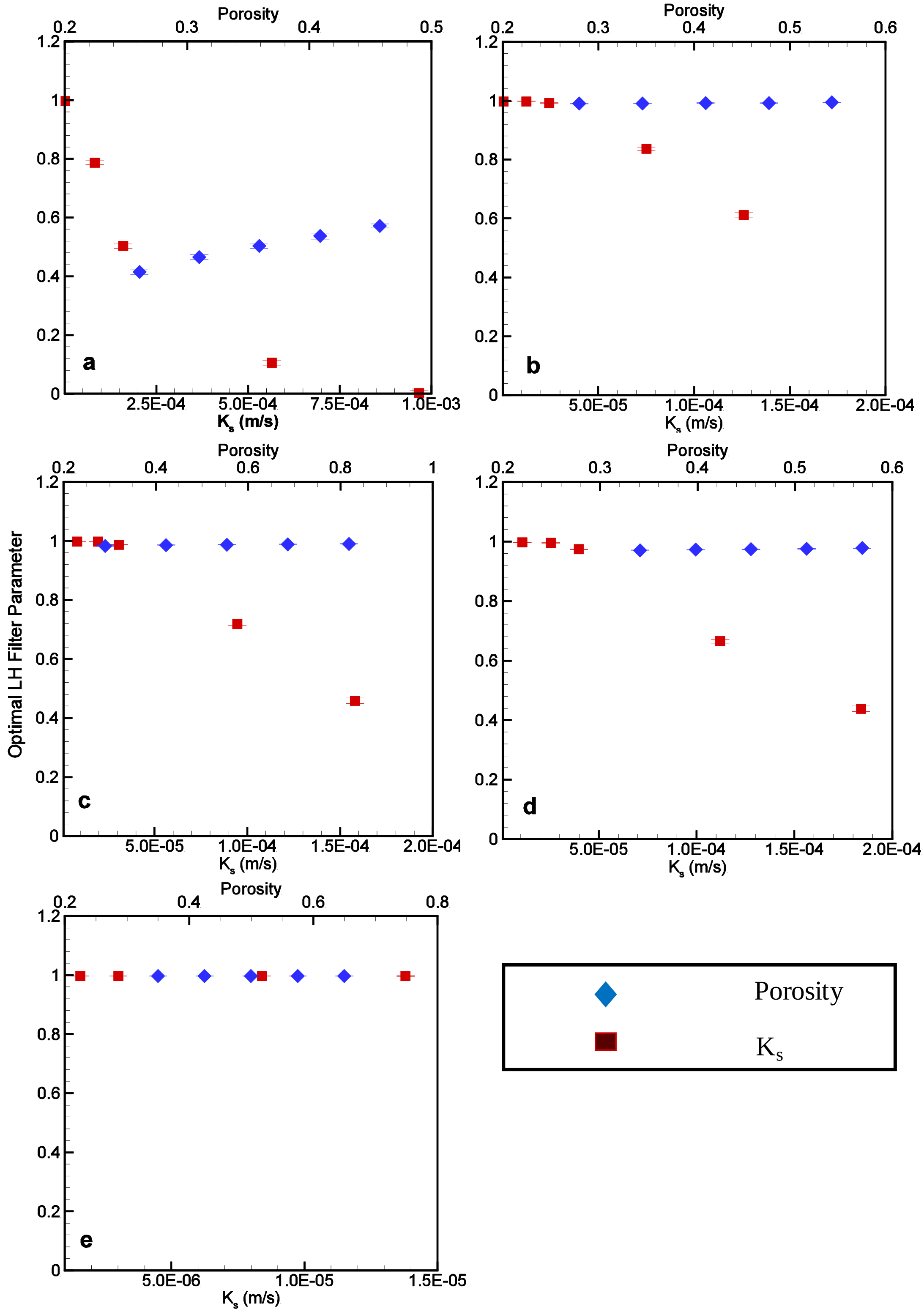

Fig. 6 Values of the optimal LH filter parameter with the error bars obtained from the linear estimates of uncertainty for sand (a), sandy loam (b), loam (c), loamy sand (d) and silt loam (e) with different soil properties

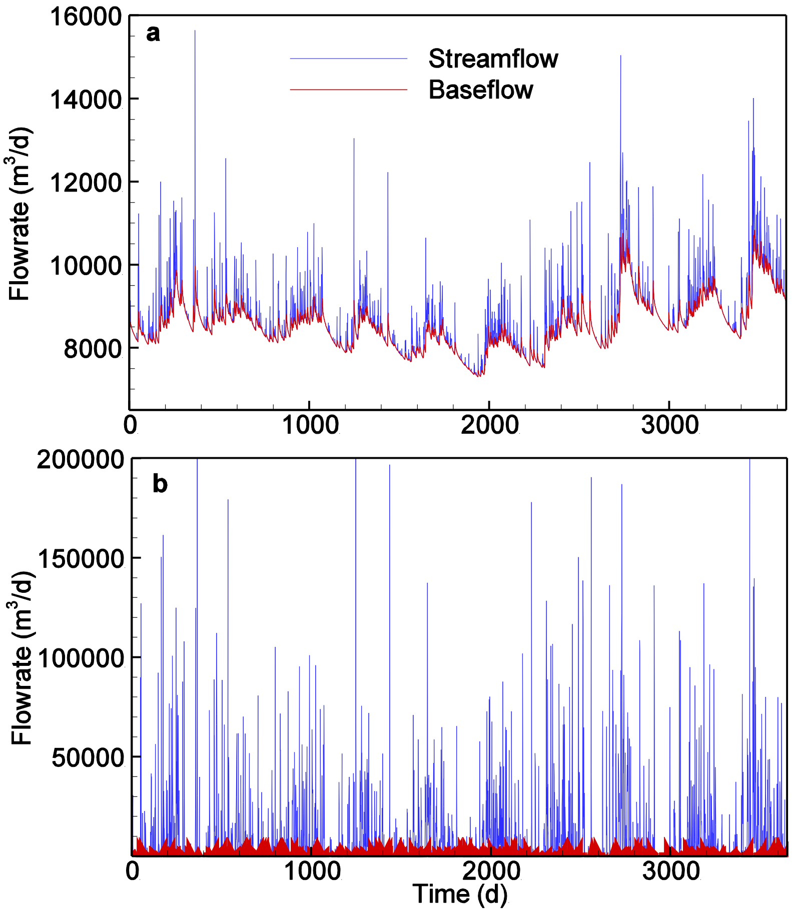

Fig. 7 Simulated streamflow and baseflow for catchments with sand (a) and silt loam (b) with their mean values of K_s and porosity

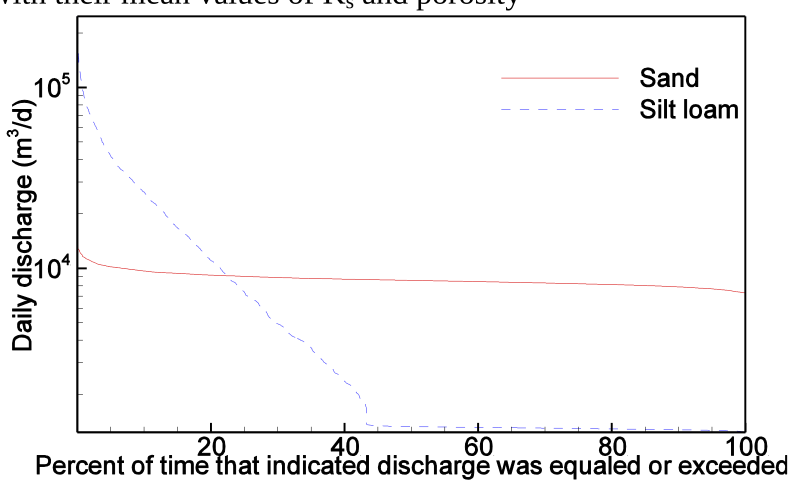

Fig. 8 Flow duration curves for catchments with sand and silt loam with their mean values of K_s and porosity

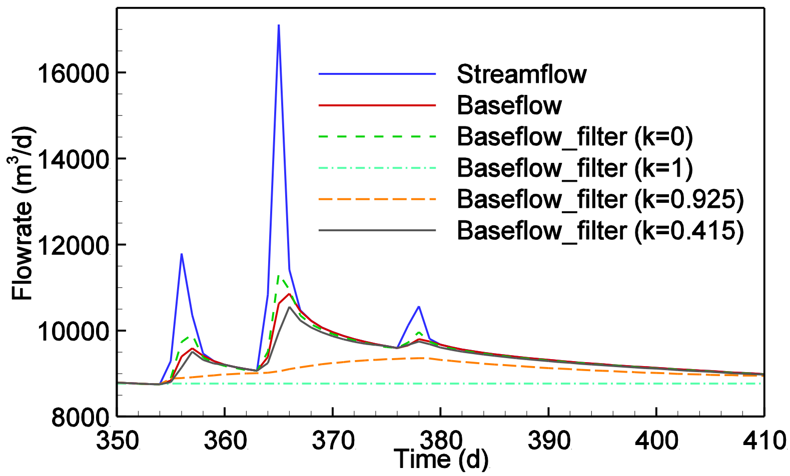

Fig. 9 Impact of different values of LH filter parameter on baseflow for catchment with sand with minimum porosity

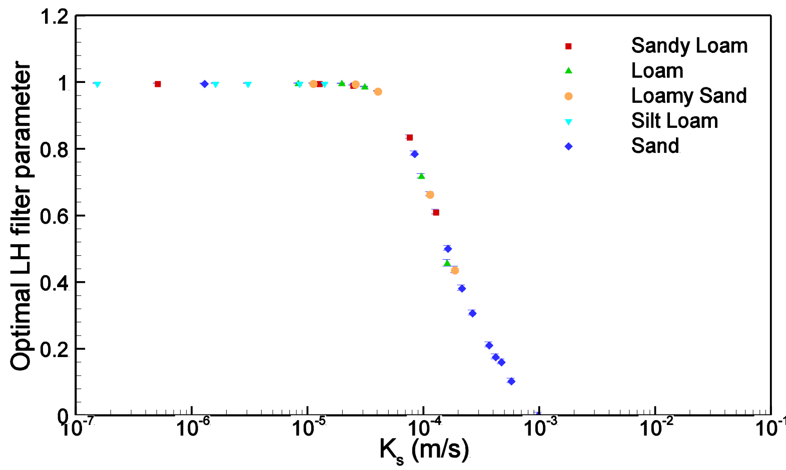

Fig. 10 Relationship between the optimal LH filter parameter and K_s with the error bars obtained from the linear estimates of uncertainty for different soil properties

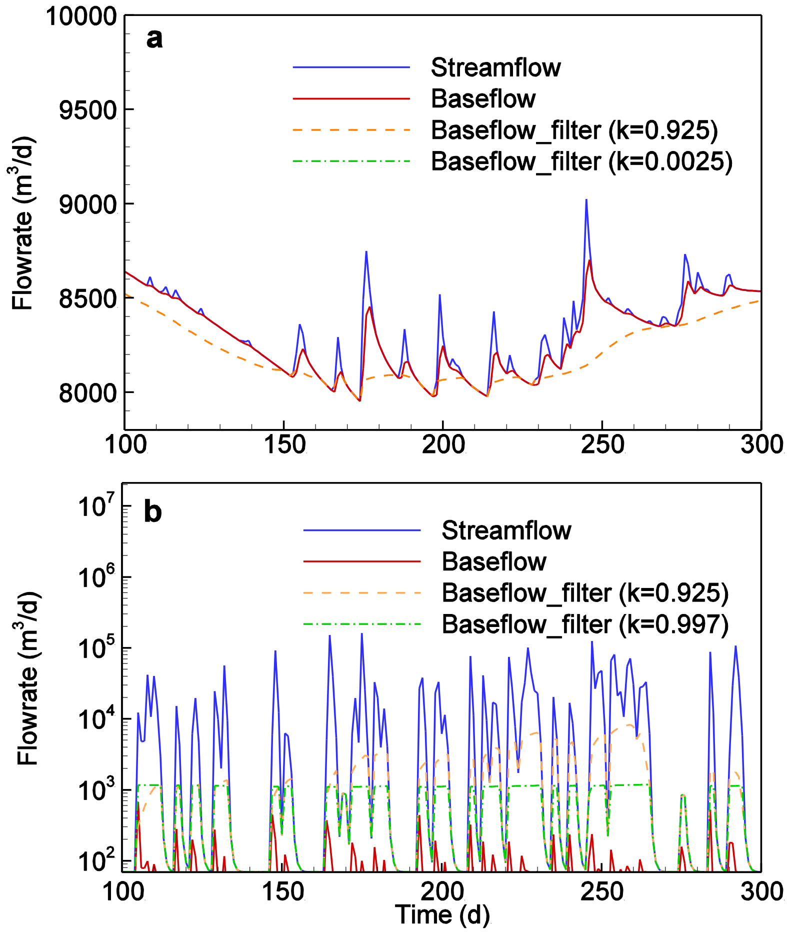

Fig. 11 Comparison of baseflow calculated from the HGS model simulation and the LH filter with two different values of the filter parameter for sand with maximum K_s (a) and silt loam with minimum K_s (b)

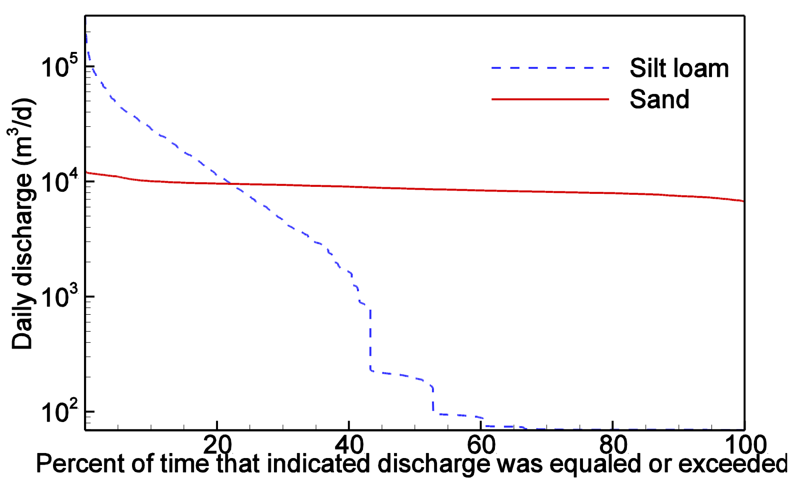

Fig. 12 Flow duration curves for catchments with sand with maximum K_s and silt loam with minimum K_s

1.19 *Page 26, figure 10: I still find it remarkable that most points fall onto a line. The response to the previous point 1.3 of reviewer 1 does not bring along any explanations.*

Response: The reason for this relationship is discussed in Section 4.1 of the paper, which has now been made clearer. In particular, the following paragraphs have been modified significantly to provide this explanation more explicitly (starting on lines 422 and 429):

> "As discussed above, larger values of K_s result in larger baseflow and vice versa, and as discussed in Section 3.3 and shown in Fig. 9, for a catchment with sandy soil, smaller values of the LH filter parameter result in larger baseflow contributions and vice versa. Consequently, there exists an inverse relationship between K_s and the optimal LH filter parameter values, as shown in Fig. 6."

> "To further confirm the inverse relationship between K_s and the optimal value of the LH filter parameter, five additional simulations (i.e. generation of simulated streamflow and baseflow using HGS, optimization of the LH filter parameter and the determination of filtered baseflow) were conducted with K_s values between the mean and upper quartile values of K_s for sand. The results obtained for all of the simulations conducted are shown in Fig. 10, including the linear estimates of uncertainty, which are very small, indicating that the results obtained can be treated with confidence. As can be seen, the additional results confirm the strong inverse relationship between the optimal value of the LH filter parameters and K_s, regardless of soil type, which is as expected, based on the discussion of the impact of K_s on baseflow and the way different filter parameter values affect the output from the LH filter given above. However, as can be seen from Fig. 10, the optimal values of the LH filter parameter are almost constant very close to their maximum value of 1.0 for soils with small values of K_s, suggesting that for small values of K_s, baseflow estimates obtained using the LH filter might be inaccurate, as baseflow decreases with decreasing values of K_s, while the baseflow hydrographs obtained using the LH filter remain constant (also see Section 4.2)."

1.20 *Page 25, line 53: what is small, the parameters or uncertainties?*

Response: It is assumed that the reviewer was referring to line 28/29 of page 18 of the PDF version. This sentence has been amended to make the explanation clearer and now reads (starting from line 432):

> "The results obtained for all of the simulations conducted are shown in Fig. 10, including the linear estimates of uncertainty, which are very small, indicating that the results obtained can be treated with confidence."

1.21 *Are the figure axis of 7 and 11 correct? I was wondering why for example there is 10 times more flow in the sand in figure7, or nearly 100 times more in figure 11. In the end, the amount of rainfall is the same in both cases.*

Response: The axes in figures 7 and 11 are correct in the manuscript. Although the reviewer is correct to point out that the shape of these two streamflow hydrographs, either in Figure 7 or in

Figure 11, look very different with the same amount of rainfall input, the total amount of the streamflow for these two cases is similar to each other, with similar integrated areas over the streamflow hydrographs. The reason why the streamflow hydrograph shapes look so different is because under the same rainfall, the catchment with sandy soil has a larger value of K_s, and most of the rainfall infiltrates into the ground and becomes groundwater, leading to a large baseflow contribution in the absence of rainfall. Therefore, the streamflow hydrograph for this soil has a lower proportion of surface runoff and a higher proportion of baseflow. For the catchment with silt loam, which has a smaller K_s, rainfall cannot infiltrate easily, but is converted to surface runoff, rapidly feeding the stream, and thus this catchment has streamflow with a higher peak, with almost no baseflow contribution.

<u>1.22</u> W*hy is the x- axis in fig. 11 different for the two plots?*

<u>Response:</u> Figure 11 has been redrawn with the same x- axis and can be seen in response to comments <u>1.17&1.18.</u>

<u>1.23</u> *Summary and conclusions: delete "research studies to be conducted in order to" from the second sentence.*

<u>Response:</u> The authors think "research studies to be conducted" should be kept in this sentence, because it was included to make it clear that it is not intended to use the framework each time a filter is used to obtain baseflow estimates, which was in response to this reviewer's comment in the first round of reviews.

<u>1.24</u> *Finally, I am not sure if I would end the paper with a long discussion (exceeding the length of the conclusions listed in the second paragraph) on why the results must be treated with care.*

<u>Response:</u> This was in response to another reviewer and is important in order to point out the limitations of the study.

<u>Reviewer #2 comments:</u>

<u>2.1</u> *Overall, I am satisfied with the revision of the manuscript. The only item of concern is the authors justification for use of coefficient of efficiency (page 60). That is, I don't think it is sufficient to justify an adoption of a measure of model performance simple because many others have used it. Moving on from this minor issue, what I was trying to communicate in my review was that the coefficient of efficiency should be considered as an aggregation of multiple objective functions. When considered as such many interesting aspects of the model may become detectable. I urge the authors to re-read Gupta et al. (2011) and also to read Gupta et al. (2009).*
Gupta, H.V., Kling, H., 2011. On typical range, sensitivity, and normalization of mean squared error and Nash-Sutliffe efficiency type metrics. Water resources research 47(10) W1061
Gupta, H.V., Kling, H., Yilmaz, K., and Martinez, G. (2009), Decomposition of the mean squared error and NSE performance criteria: Implications for improving hydrological modelling, J. Hydrol., 377(1-2), 80-91.

Response: The reviewer is correct in suggesting that by regarding the coefficient of efficiency (E_f) as an aggregation of multiple objective functions, many aspects of the model may be detectable, as discussed in Gupta and Kling (2011) and Gupta et al. (2009). However, the authors believe that the original E_f (Nash and Sutcliffe, 1970) is sufficient to be used as an error measure for this study. This is because the variability in the baseflow hydrograph derived from the LH filter is quite constrained and only affected by the value of a single model parameter. As the impact of the value of the parameter on the baseflow hydrograph is well understood, as discussed in the paper (i.e. low values of the LH filter parameter increase the peak in the baseflow hydrograph and vice versa), the reasons for poor filter performance can be diagnosed easily, as was done in the discussion of the results. This has now been made clear in the manuscript (starting line 342):

> "The dimensionless coefficient of efficiency (E_f) was used as the error measure for evaluating the performance of filters with different parameters and applied to catchments with different soil conditions. This is because it is one of the most commonly used error measures in hydrology and provides a trade-off between objectives that emphasize different aspects of hydrographs (Gupta and Kling, 2011; Gupta et al., 2009). However, it should be noted that because of the nature of the LH filter, constraints are placed on the variability of the resulting baseflow hydrograph. For example, as discussed previously, the timing of the peak of the baseflow hydrograph always coincides with the timing of the peak of the total streamflow hydrograph and whenever baseflow is larger than the total streamflow, baseflow is forced to be equal to the total streamflow, thereby capturing the recession limb of the baseflow hydrograph. As a result, the only variability is in the magnitude of the baseflow hydrograph, which is controlled by the LH filter parameter, as discussed above (i.e. smaller values of the filter parameter result in larger peaks and vice versa)."

It should be noted that the impact of using the decomposed version of E_f under typical (optimized) situation (Gupta and Kling, 2011) for calibration was tested and found to have an insignificant impact on the optimal filter parameters for the reasons described above. In addition, it provided no additional insight into the causes of poor filter performance, as filter behaviour is solely affected by model structure and the value of a single parameter and is therefore predictable. The filter performed poorly at extreme values of the possible range of filter parameter values, suggesting that the filter is not suitable (i.e. there are structural inadequacies in the model) in these cases, as discussed in the paper. However, the decomposition will most likely be useful in future work, which is focused on the comparison of the performance of different filters. As a result, the description of E_f as the performance measure has been removed from the description of the general methodology (Section 2.1) and replaced with a more generic discussion about possible error measures, as follows (starting from line 157):

> "This comparison can be carried out using a number of different evaluation measures, such as the mean square error (MSE), Nash-Sutcliffe coefficient of efficiency (E_f) (Nash and Sutcliffe, 1970), percent bias (PBIAS) (Guttal and Jayaprakash, 2009) or the decompositions of MSE and E_f (Gupta and Kling, 2011; Gupta et al., 2009), among others. The choice of which measures are most appropriate is case study dependent (e.g.

whether accurate estimation of the peak, timing or volume of the baseflow hydrograph is most important)."

The corresponding information in Section 2.2 has also been changed as follows (starting from line 176):

"Any of the performance measures mentioned in Section 2.1 can be used for this purpose. Alternatively, a multi-objective approach can be adopted (e.g. Gibbs et al., 2012)."

The details of using E_f as the error measure have now been moved into the case study section (Section 3.4, starting from line 342):

"The dimensionless coefficient of efficiency (E_f) was used as the error measure for evaluating the performance of filters with different parameters and applied to catchments with different soil conditions. This is because it is one of the most commonly used error measures in hydrology and provides a trade-off between objectives that emphasize different aspects of hydrographs (Gupta and Kling, 2011; Gupta et al., 2009). However, as discussed previously, it should be noted that because of the nature of the LH filter, constraints are placed on the variability of the resulting baseflow hydrograph. For example, the timing of the peak of the baseflow hydrograph always coincides with the timing of the peak of the total streamflow hydrograph and whenever baseflow is larger than the total streamflow, baseflow is forced to be equal to the total streamflow, thereby capturing the recession limb of the baseflow hydrograph. As a result, the only variability is in the magnitude of the baseflow hydrograph, which is controlled by the LH filter parameter, as discussed above (i.e. smaller values of the filter parameter result in larger peaks and vice versa).

The equation of E_f was given by Nash and Sutcliffe (1970) as:

$$E_f = 1 - \left[\frac{\sum_{i=1}^{n} (Y_i^{obs} - Y_i^{sim})^2}{\sum_{i=1}^{n} (Y_i^{obs} - Y^{mean})^2} \right] \tag{9}$$

where Y_i^{obs} is the ith observation of the flow rate being evaluated [LT^{-1}], Y_i^{sim} is the ith simulated value of the flow rate being evaluated [LT^{-1}], Y^{mean} is the mean of the observed data for the flow rate being evaluated [LT^{-1}], i is the time step [T], and n is the total number of observations.

When using E_f to evaluate the performance of RDFs, the observed data in equation (9) are given by the simulated baseflow results obtained from the fully integrated SW/GW model (q_b^{sim}), while the baseflow results derived from the RDFs (q_b^{filter}) correspond to the simulated values. Based on benchmark values available from other studies (Herron and Croke, 2009; Moriasi et al., 2007; Nejadhashemi et al., 2007), RDF performance can be judged as 'perfect' when E_f=1.0, while E_f values between 0.5 and 1.0 correspond to 'good' filter performance; E_f values between 0.0 and 0.5 show 'acceptable' filter performance and ‘unacceptable’ filter performance is represented by negative values of E_f.

In order to estimate the uncertainty associated with estimates of the optimal LH filter parameters, the following linear estimate of uncertainty was used (Vugrin et al., 2005):

$$\left\{ k : \frac{S(k) - S(\hat{k})}{S(\hat{k})} \leq \frac{p}{n-p} F^{\alpha}_{p,n-p} \right\} \tag{10}$$

$$S(k) = \sum_{i=1}^{n} [q^{filter}_{b(i)}(k) - q^{sim}_{b(i)}]^2 \tag{11}$$

where $\hat{k}$ is the optimal LH filter parameter, obtained by minimizing the sum of squared errors between the baseflow obtained from the LH filter and that simulated using the HGS model (Eq. 11); p is the number of parameters to be estimated, which is 1 in this case; n is the number of data points, which is 3650 days in this case; and $F^{\alpha}_{p,n-p}$ is the upper α percent point of the F-distribution, which was set to 0.05.

The optimization method used in order to obtain the optimal values of the filter parameters was the golden section search method (Press et al., 1992), as there was only one model parameter.”

Suggested Reviewer List (include up to 5 names and their contact details)

Suggested Reviewers

1. Rene Therrien – rene.therrien@ggl.ulaval.ca
2. Philip Brunner – Philip.brunner@unine.ch
3. Tim Peterson – timjp@unimelb.edu.au
4. Frank Schwartz – Schwartz.11@osu.edu
5. Ed Sudicky – sudicky@sciborg.uwaterloo.ca

***Highlights (for review)**

- Generic frameworks for using fully integrated surface water/ground water (SW/GW) models for assessing and improving the performance of recursive digital filters (RDFs) used for baseflow estimation are introduced.
- RDF performance can be improved by calibrating the filter parameter(s) by taking catchment characteristics and hydrological inputs into account.
- The frameworks were applied to a hypothetical case study, using HydroGeoSphere (HGS) for assessing and improving the Lyne and Hollick (LH) filter for a range of soil properties, and the results obtained compared with those obtained using the commonly used value of the filter parameter of 0.925.
- Case study results suggest that LH filter performance and the optimal value of the filter parameter is affected significantly by the saturated hydraulic conductivity (K_s) and use of the calibrated LH filter parameter can result in significant improvements in filter performance.

Framework for Assessing and Improving the Performance of Recursive Digital Filters for Baseflow Estimation with Application to the Lyne and Hollick Filter

Li L.[a], Maier H.R.[a], Lambert M.F.[a], Simmons C.T.[b], Partington D.[a]

a. School of Civil, Environmental and Mining Engineering, The University of Adelaide, Adelaide, South Australia, 5005, Australia

lli@civeng.adelaide.edu.au Tel: +61 (0)8 8313 4323

holger.maier@adelaide.edu.au Tel: +61 (0)8 8313 4139

martin.lambert@adelaide.edu.au Tel: +61 (0)8 8313 4320

daniel.partington@adelaide.edu.au Tel: +61 (0)8 8313 4323

Fax: +61 (0)8 83034359

b. National Centre for Groundwater Research and Training and School of the Environment, Flinders University, GPO Box 2100, Adelaide, South Australia, AUSTRALIA 5001

craig.simmons@flinders.edu.au Tel: (+61 8) 8201 5509

Fax: (+61 8) 8201 7906

Key Words: baseflow estimation; fully integrated surface water/ground water model; digital filters, framework

Abstract

Baseflow is often regarded as the streamflow component derived predominantly from groundwater discharge. The estimation of baseflow is important for water supply, water allocation, investigation of contamination impacts, low flow hydrology and flood hydrology. Baseflow is commonly estimated using graphical methods, recursive digital filters (RDFs), tracer based methods, and conceptual models. Of all of these methods, RDFs are the most commonly used, due to their relatively easy and efficient implementation. This paper presents a generic framework for assessing and improving the performance of RDFs for baseflow estimation for catchments with different characteristics and subject to different hydrological conditions. As part of the framework, a fully integrated surface water/groundwater (SW/GW) model is used to obtain estimates of streamflow and baseflow for catchments with different properties, such as soil types and rainfall patterns. A RDF is then applied to the simulated streamflow to assess how well the baseflow obtained using the filter matches the baseflow obtained using the fully integrated SW/GW model. In order to improve the performance of the filter, the user-defined parameter(s) controlling filter

operation can be adjusted in order to obtain the best match between the baseflow obtained using the filter and that obtained using the fully integrated SW/GW model (i.e. through calibration). The proposed framework is tested by applying it to a common SW/GW benchmarking problem, the tilted V-catchment, for a range of soil properties. HydroGeoSphere (HGS) is used to develop the fully integrated SW/GW model and the Lyne and Hollick (LH) filter is used as the RDF. The performance of the LH filter is assessed using the commonly used value of the filter parameter of 0.925, as well as calibrated filter parameter values. The results obtained show that the performance of the LH filter is affected significantly by the saturated hydraulic conductivity (K_s) of the soil and that calibrated LH filter parameter can result in significant improvements in filter performance.

1. Introduction

Baseflow is often defined as the groundwater contribution to streamflow, however it is also referred to as slow flow, and sustained flow (Hall, 1968). Herein, the former definition of baseflow is adopted, i.e. the groundwater contribution to a stream. The estimation of baseflow can play a significant role in terms of understanding the interaction between surface water and groundwater (Evans and Neal, 2005; Gilfedder et al., 2009). In addition, baseflow estimation is important for a wide range of water and environmental management issues, such as water supply, water allocation, investigation of contamination impacts, low flow hydrology and flood hydrology (Linsley et al., 1988). One important application is the estimation of the baseflow index (BFI), which is the long term ratio of the volume of baseflow to total streamflow volume. This index was developed by the Institute of Hydrology (now

CEH Wallingford), and was used in the UK Hydrometric Register, a comprehensive reference source to help assess the low flow characteristics of rivers and the catchment geology of the UK (Marsh and Hannaford, 2008).

There is no easy way to continuously and accurately measure baseflow in the field (Dukic, 2006; McCallum et al., 2010). In the early twentieth century, the focus of baseflow estimation methods was primarily on graphical separation methods, including the constant discharge, constant slope and concave methods (Linsley et al., 1988). Although these methods are able to capture the perceived understanding of the underlying physical processes (Bako and Hunt, 1988; Sloto and Crouse, 1996), their application is subjective in terms of the choice of appropriate starting and inflexion points. Since the 1980s, researchers have developed alternative baseflow separation algorithms by using automated techniques, such as recursive digital filters (RDFs) (Arnold et al., 1995; Nathan and McMahon, 1990). These methods regard total streamflow as being composed of both quickflow and baseflow and apply signal processing techniques to a streamflow time series in order to remove the high-frequency quickflow signal to obtain the low-frequency baseflow signal. These RDFs are computationally efficient, easily automated, and can be applied to long continuous streamflow records. However, RDFs do not take into consideration the physical processes responsible for baseflow generation as their inputs, but are simply based on streamflow records and user-defined filter parameters. In addition, filters are often constrained by the condition that baseflow must not exceed total streamflow or become negative (Furey and Gupta, 2001). Environmental isotopes and chemical tracers have also been utilised for streamflow separation by using end member mixing analysis (Chapman and Maxwell, 1996;

McCallum et al., 2010; Murphy et al., 2009). These isotope and tracer approaches can be used to infer the various sources of streamflow, such as groundwater, interflow and direct rainfall. However, any uncertainty in the end member concentrations of these flow sources directly relates to the uncertainty of quantifying the groundwater component of streamflow (Jones et al., 2006; McCallum et al., 2010).

Recently, greater attention has been given to physically based approaches for analysing baseflow, including fully integrated surface water/ground water (SW/GW) flow models, such as InHM (VanderKwaak and Loague, 2001), MODHMS (HydroGeoLogic, 2000), HydroGeoSphere (HGS) (Therrien et al., 2009) and ParFlow (Kollet and Maxwell, 2006). With precipitation, evapotranspiration (ET) and parameters representing catchment characteristics as inputs, these complex, spatially distributed models can simulate both surface flow and baseflow and give a more detailed physical representation of the processes of SW/GW interaction (Khan et al., 2009; Partington et al., 2011; Ravazzani et al., 2011). In order to enable the baseflow component of streamflow to be extracted accurately from such models, Partington et al. (2011) developed a hydraulic mixing-cell (HMC) method, which accounts for stream losses and time lags within the catchment. Consequently, use of the HMC method in conjunction with fully integrated SW/GW models is likely to provide the most accurate means of estimating baseflow. However, the complexity of these models (e.g. the number of parameters that need to be obtained through calibration) requires increased data and computational resources, which make them exceedingly difficult to calibrate and apply to real catchments.

RDFs are currently the most widely used method for estimating baseflow around the world, due to their minimal input requirements and simple and efficient implementation. Such filters include the Lyne and Hollick (LH) filter (Lyne and Hollick, 1979; Nathan and McMahon, 1990), Chapman one-parameter algorithm (Chapman and Maxwell, 1996), Boughton two-parameter algorithm (Chapman, 1999), Eckhardt two-parameter algorithm (Eckhardt, 2005) and IHACRES three-parameter algorithm (Chapman, 1999). However, while there have been many studies comparing the performance of RDFs (Chapman, 1999; Eckhardt, 2005, 2008; Murphy et al., 2009; Nejadhashemi et al., 2003; Nejadhashemi et al., 2009; Partington et al., 2012), the relative performance of different RDFs cannot be assessed in absolute terms, as baseflow cannot be measured easily (Dukic, 2006; McCallum et al., 2010). This also makes it difficult to know which filters to select for particular applications.

This problem is compounded by the fact that RDFs operate solely on the total streamflow hydrograph, without considering potential impacts of physical catchment characteristics. However, by considering the hydrological processes driving baseflow, one might expect that physical catchment characteristics have a significant impact on baseflow. For example, if the rainfall rate over a dry catchment with sandy soils is smaller than the rate of infiltration, direct runoff from the surface will be very small, and the baseflow contribution to streamflow significant. On the other hand, if soils are clayey and the antecedent moisture content is high, most of the streamflow will consist of overland flow, with little contribution from baseflow. Consequently, it is likely that the performance of RDFs will vary, depending on physical catchment characteristics. However, at present, it is difficult to assess this.

The performance of RDFs is also affected by one or more user-defined parameters, which are used to change the amount of attenuation in the low/high-frequency domain of the flow spectrum, and therefore have an impact on the baseflow hydrograph obtained. However, determining appropriate values of these parameters is not straightforward and a range of values has been suggested in the literature. For example, in relation to the LH filter, Lyne and Hollick (1979) suggested that a filter parameter between 0.75 and 0.9 should be used. Arnold et.al. (1995) and Nathan and McMahon (1990) recommended using a filter parameter of 0.925. Mau and Winter (1997) found a value of 0.85 to be most appropriate and Tan et al. (2009a) suggested using the recession constant as the filter parameter value, which varies from catchment to catchment. Common to all of these studies was the goal of choosing 'suitable' filter parameters in order to obtain a better match between the baseflow obtained using the LH filter and that obtained using traditional methods of baseflow separation, such as manual graphical baseflow separation methods. However, as there is no objective way of assessing how well RDFs predict actual baseflow, it is difficult to know which of the suggested values should be used. In addition, even though many authors have attempted to find an optimal value of the LH filter parameter that can be applied to all catchments, adjusting filter parameter values for different types of catchments is particularly important, as even a modest change in the LH filter parameter can result in an almost 100% change in baseflow for more ephemeral streams, for example. While the need to adjust filter parameters for catchments with different physical properties has been recognized for some RDFs, such as the Boughton two-parameter algorithm (Chapman, 1999) and the Eckhardt filter method (Eckhardt, 2005), there is still a need to develop a generic approach for determining appropriate values of these filter parameters and to assess the impact these values have on filter performance for various catchments with different physical properties.

In order to address the shortcomings in filter based baseflow estimation outlined above, a generic framework for assessing and improving the performance of RDFs is introduced in this paper. The proposed framework enables the performance of different RDFs to be assessed systematically and the optimal values of filter parameters to be determined for a range of physical catchment characteristics. In order to demonstrate the usefulness of the proposed framework, it is applied to a hypothetical case study. The remainder of this paper is organised as follows. The proposed framework is introduced in Section 2, followed by a description of the case study in Section 3. The results obtained for the case study are presented and discussed in Section 4 and a summary and conclusions are given in Section 5.

2. Generic Framework for Assessing and Improving the Performance of RDFs for Baseflow Estimation

The underlying premise of the proposed framework for assessing and improving the performance of RDFs for baseflow estimation is that fully integrated SW/GW models can be used to obtain reasonably accurate estimates of actual baseflow, thereby providing a benchmark against which the performance of RDFs can be assessed. This is a reasonable assumption, as fully integrated SW/GW models provide a rigorous representation of the underlying physical processes of hydrologic systems (Brookfield et al., 2009; Furman, 2008; Partington et al., 2012; Sulis et al., 2010; Therrien and Sudicky, 1996). While it is acknowledged that fully integrated SW/GW models are in themselves an approximation of the actual processes in real catchments, they provide the best means of quantifying the absolute volume of baseflow currently available (Ferket et al., 2010). In addition, they can be used to obtain estimates of baseflow for catchments with different characteristics. Therefore they are able to provide the first step towards being able to assess the absolute performance of RDFs under a range of physical conditions. The generic frameworks for using fully integrated SW/GW models for assessing and improving the performance of RDFs used for baseflow estimation are given in Sections 2.1 and 2.2, respectively.

2.1. Performance Assessment

The proposed framework for assessing the performance of RDFs under a range of physical catchment conditions is shown in Fig. 1. As mentioned above, the underlying premise of the proposed approach is that a fully integrated SW/GW model provides the best possible approximation to the physical processes of water flow within catchments and can therefore be used as an approximation to such processes subject to a variety of physical characteristics and forcings. This is because rainfall is allowed to partition into overland flow, streamflow, evaporation, infiltration and recharge in a physically based fashion (Therrien et al., 2009), without prior definition of flow generation processes or storage discharge relationships. All of the governing flow equations implemented by the fully integrated SW/GW model are solved simultaneously to obtain the simulated streamflow (q) and baseflow (q_b^{sim}) as a function of user-defined catchment characteristics (e.g. soil types, catchment size, catchment shapes) and hydrological inputs (e.g. rainfall patterns, antecedent moisture, evaporation) (Fig. 1).

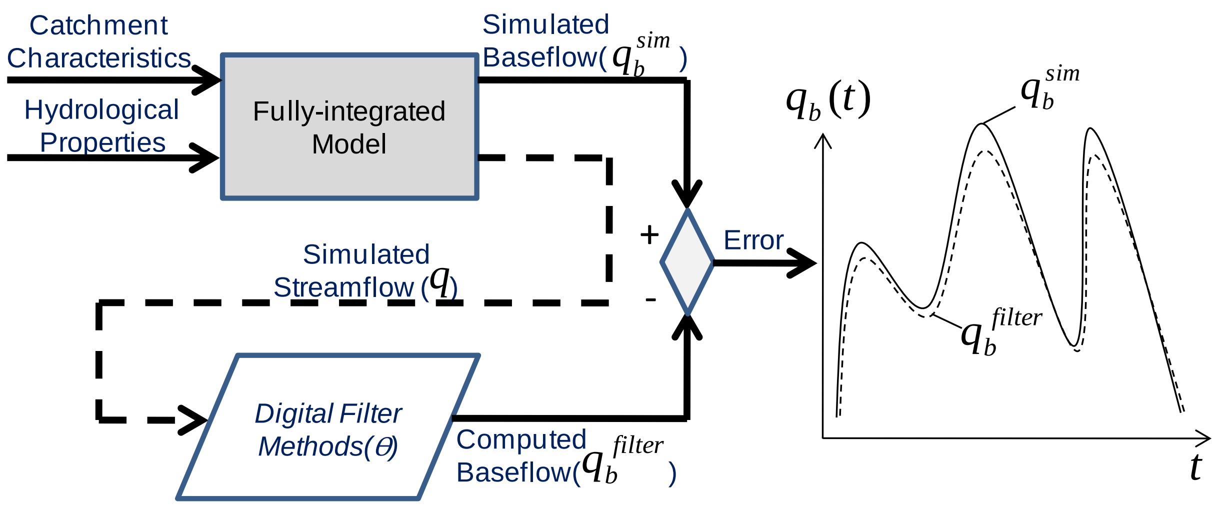

Fig. 1. Schematic description of the framework for assessing the performance of RDFs for baseflow estimation

The simulated streamflow obtained from the fully integrated SW/GW model (q) is then used as the input to the RDF in order to compute the filtered baseflow hydrograph (q_b^{filter}) (Fig. 1). The proposed framework can be used to assess the performance of any RDF. In order to assess RDF performance, the baseflow obtained with the aid of the RDF (q_b^{filter}) can be compared with the 'real' baseflow estimated using the fully integrated SW/GW model (q_b^{sim}) (Fig. 1). This comparison can be carried out using a number of different evaluation measures, such as the mean square error (MSE), Nash-Sutcliffe coefficient of efficiency (E_f) (Nash and Sutcliffe, 1970), percent bias (PBIAS) (Guttal and Jayaprakash, 2009) or the decompositions of MSE and E_f (Gupta and Kling, 2011; Gupta et al., 2009), among others. The choice of which measures are most appropriate is case study dependent (e.g. whether accurate estimation of the peak, timing or volume of the baseflow hydrograph is most important). The performance assessment of a particular filter can be repeated for different physical catchment conditions and hydrological inputs (Fig. 1), providing insight into how filter performance is affected by these factors and determining the range of conditions under which filter performance is acceptable.

2.2. Performance Improvement

As mentioned previously, the performance of RDFs is generally a function of the values of one or more user-defined parameters. Some filter parameters are simply used to alter the magnitude and shape of the resulting baseflow hydrograph, such as the parameter of the LH filter (Lyne and Hollick, 1979; Nathan and McMahon, 1990) and one of the parameters (C) of the Boughton two-parameter algorithm (Chapman, 1999), while others have some physical meaning through a relationship with the recession constant or being defined relative to some of the underlying physical processes.

In order to determine the best possible values of the filter parameters for a given catchment, the assessment framework introduced in the previous section can be extended, as shown in Fig. 2. Based on the assumption that the simulated baseflow obtained using the fully integrated SW/GW model (q_b^{sim}) is representative of the 'real' baseflow, the filter parameter(s) (θ) can be adjusted to minimize an error measure between the 'real' baseflow (q_b^{sim}) and the baseflow computed using the RDF (q_b^{filter}). Any of the performance measures mentioned in Section 2.1 can be used for this purpose. Alternatively, a multi-objective approach can be adopted (e.g. Gibbs et al., 2012). This calibration process can be automated using various optimization methods, such as gradient based methods or evolutionary algorithms, depending on the complexity of the calibration problem (e.g. the number of parameters to be estimated).

By calibrating the RDFs, it is possible to determine whether filter performance can be improved by using optimal parameter values, rather than those commonly used in the literature. In addition, optimal filter parameters can be obtained for catchments with different physical characteristics, which will assist with providing an insight into the range of catchment properties for which different RDFs are applicable (i.e. perform adequately), provided the optimal filter parameters are used (referred to as the 'range of applicability' of different RDFs) and the sensitivity of optimal values of filter parameters to various catchment properties.

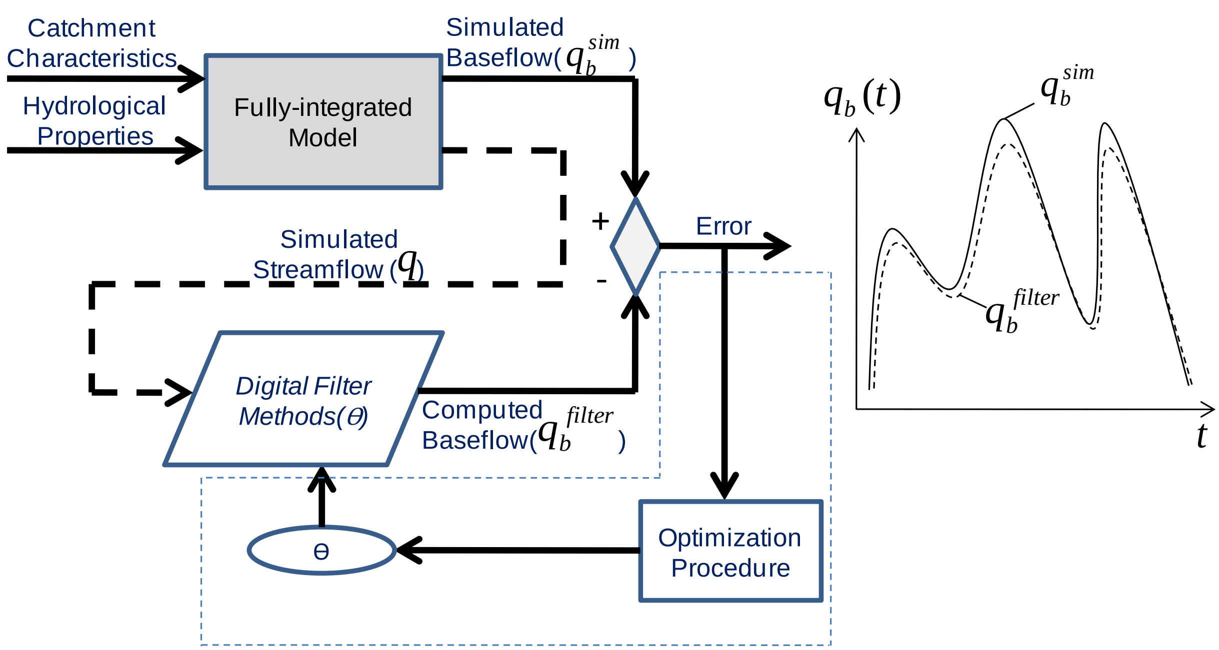

Fig. 2. Schematic description of the framework for improving the performance of RDFs for baseflow estimation

3. Case Study

In this section, a case study is used to illustrate the benefits of the proposed frameworks. The various components of the frameworks (Fig. 1 and Fig. 2) in relation to the case study are discussed in detail below.

3.1. Catchment Characteristics and Hydrological Properties

The hypothetical catchment used in this study (shown in Fig. 3) is loosely based on a common SW/GW benchmarking problem, the tilted V-catchment of Panday and Huyakorn (2004), which is based on DiGiammarco et al. (1996). Due to symmetry, the geometry of only half of the catchment is described here. The catchment is modified from the catchment given in Panday and Huyakorn (2004) in the following ways: The large slopes perpendicular and parallel to the channel have been reduced from 0.05m/m and 0.02m/m to 0.02m/m and 0.01m/m, respectively, in order to create a greater spatial distribution of the surface-subsurface exchanges throughout the catchment. The areal extent of the catchment has been increased from 810,000m^2 to 6,030,000m^2, by enlarging the original length (y direction) and width (x direction) of the catchment from 1000m and 810m to 3000m and 2010m, respectively. In order to obtain continuous baseflow contributions to the stream, the stream width was retained at 10m as in the original catchment, which can reduce the boundary effects and increase aquifer storage capacity.

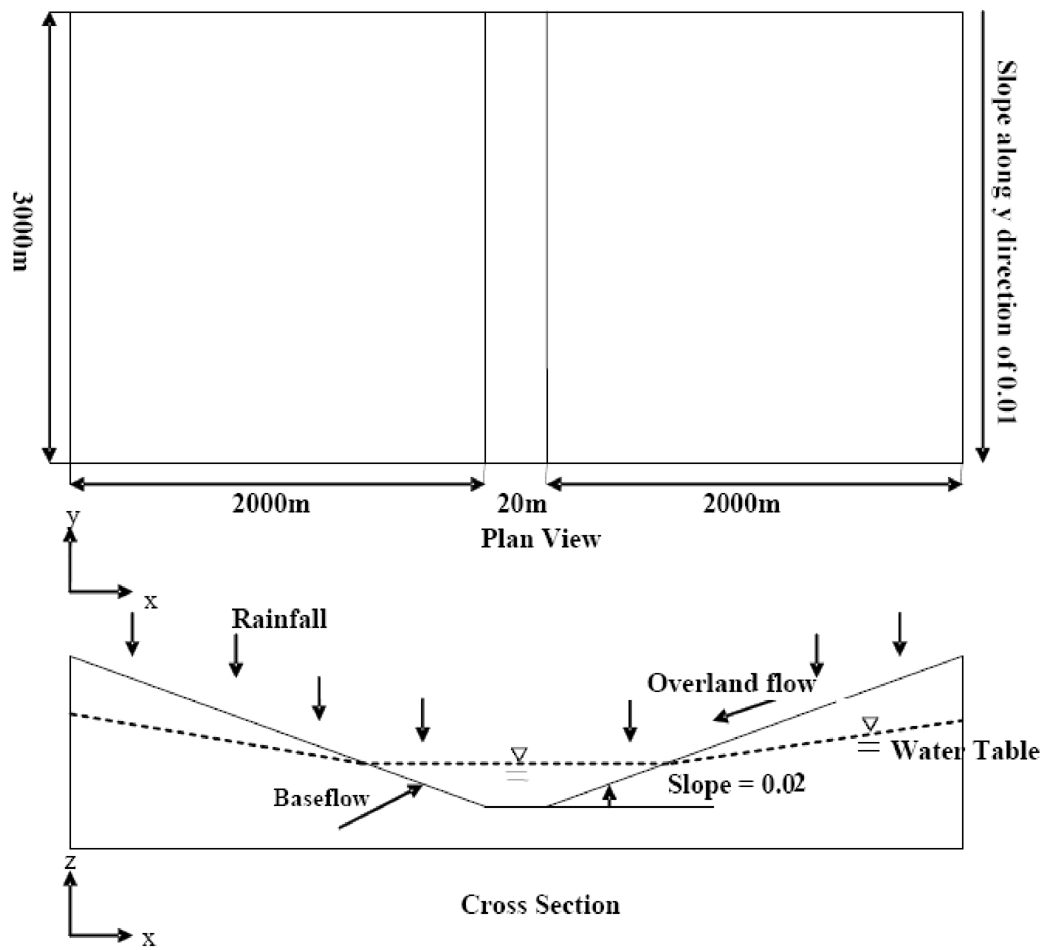

Fig. 3. Schematic Representation of Tilted V-Catchment Flow Problem (Refer to Panday and Huyakorn (2004))

The underlying aquifer extends to a depth of 20m below the stream outlet location, and is homogenous and isotropic. Five different homogeneous soil types are considered, which are characterized by different values of saturated hydraulic conductivity (K_s), porosity, residual water content (θ_r), and van Genuchten parameters α and N(β). The ranges and mean values of the soil parameters used are shown in Table 1, which were taken from Puhlmann et al. (2009). A typical ten year period of daily rainfall data from Adelaide, South Australia was used as hydrological input for illustration purposes, which is shown in Fig. 4. In view of the small size of the catchment studied, rainfall intensities have been assumed to be spatially uniform. It should be noted that only the geometry of the catchment is based on the original test case presented in Panday and Huyakorn (2004), and that the other parameters, such as soil types and rainfall patterns, are described as above.

Table 1 Soil types and ranges and means (shown in brackets) of soil properties considered for model simulations (taken from Puhlmann et al. (2009))

Soil Type	Porosity	θ_r	K_s (m/s)	α (m^{-1})	N(β)
Sand	0.261-0.4578 (0.359)	0-0.0072 (0.004)	1.27E-6-9.66E-4 (1.6E-4)	0.572-16.412 (8.492)	1.32-8.52 (4.92)
Sandy loam	0.28-0.544 (0.412)	0-0.22 (0.108)	5.01E-7-1.26E-4 (2.44E-5)	0.47-11.75 (6.11)	1.2-5.16 (3.18)
Loam	0.29-0.818 (0.554)	0-0.456 (0.228)	6.31E-7-1.58E-4 (3.07E-5)	0.68-14.56 (7.418)	1.0822-2.252 (1.682)
Loamy sand	0.341-0.569 (0.455)	0-0.1584 (0.079)	1.42E-6-1.84E-4 (3.99E-5)	0.544-17.344 (8.944)	1.2821-2.2661 (1.774)
Silt loam	0.35-0.65 (0.5)	0-0.3 (0.15)	1.51E-7-1.38E-5 (3.01E-6)	0.18-10.98 (5.58)	1.15-3.55 (2.35)

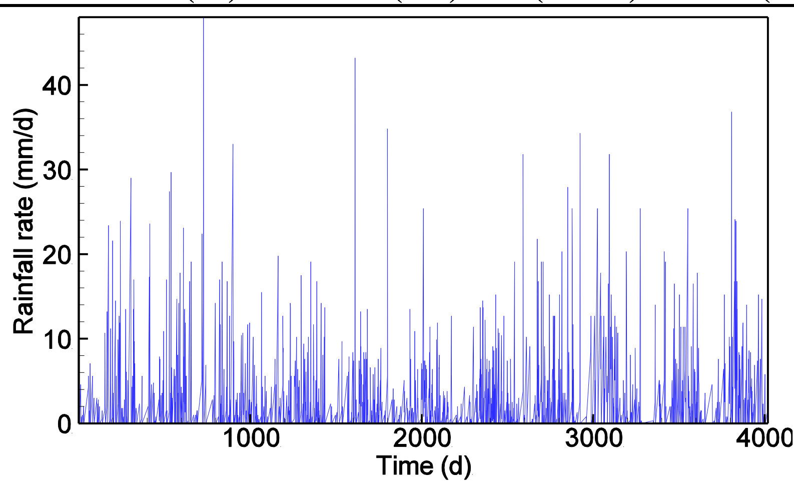

Fig. 4 Ten year daily rainfall data for Adelaide, South Australia, gauge number 23000

3.2. Fully integrated SW/GW Model

HydroGeoSphere (HGS) was used as the fully integrated SW/GW model. HGS was considered suitable for this application, as it represents the physical catchment processes explicitly. This is because HGS can solve the equations for both surface and variably-saturated subsurface flow regimes at each time step simultaneously, which results in realistic, physically-based simulation of the movement of water on and within catchments (Therrien et al., 2009). HGS has been applied successfully to losing/gaining stream analysis (Partington et al., 2011), SW/GW disconnection problems (Banks et al., 2011; Brunner et al., 2009), the dynamics of river bank storage processes (Doble et al., 2012) and dual permeability systems (Schwartz et al., 2010).

HGS uses the diffusion wave approximation to the 2D St. Venant equations to simulate surface flow (Therrien et al., 2009):

$$\frac{\partial \phi_0 h_0}{\partial t} - \frac{\partial}{\partial x}(d_0 K_{ox} \frac{\partial h_0}{\partial x}) - \frac{\partial}{\partial y}(d_0 K_{oy} \frac{\partial h_0}{\partial y}) + d_0 \Gamma_0 \pm Q_0 = 0 \qquad (1)$$

where ϕ_0 is the surface flow domain porosity; d_0 is the depth of water above the surface [L]; Γ_0 is the volumetric fluid exchange rate with the subsurface [LT^{-1}]; h_0 is the water surface elevation related to the datum [L] ($h_0 = d_0 + z_0$, where z_0 is the bed/land surface elevation [L]); Q_0 is a volumetric flow rate per unit area representing external sources and sinks [LT^{-1}]. All of the above symbols represent state variables, except for K_{ox}

and K_{oy}, which are parameters representing surface conductance in the x- and y- directions [LT^{-1}] and can be calculated by Manning's equation or the Chezy equation.

The following modified Richard's equation is applied for subsurface flow (Therrien et al., 2009):

$$-\nabla \cdot (-\overline{K} \cdot k_r \nabla(\psi + z)) + \sum \Gamma_{ex} \pm Q = \frac{\partial}{\partial t}(\theta_s S_\omega) \tag{2}$$

where $\overline{K}$ is the hydraulic conductivity tensor [LT^{-1}]; k_r is the relative permeability; ψ is the pressure head [L]; z is the elevation head [L]; Γ_{ex} is the volumetric subsurface fluid exchange rate with the surface domain [$L^3L^{-3}T^{-1}$]; Q is a volumetric fluid flux per unit volume representing a subsurface source or sink [$L^3L^{-3}T^{-1}$]; θ_s is the saturated water content and S_ω is the degree of water saturation.

The degree of saturation can be determined by the Van Genuchten equations (Van Genuchten, 1980):

$$S_\omega = S_{\omega r} + (1 - S_{\omega r})[1 + |\alpha\psi|^\beta]^{-\nu} \quad \text{for} \quad \psi < 0 \tag{3}$$

$$S_\omega = 1 \qquad \text{for} \quad \psi > 0 \tag{4}$$

$$\nu = 1 - \frac{1}{\beta} \qquad \text{for} \quad \beta > 1 \tag{5}$$

where $S_{\omega r}$ is the residual water saturation, and α, β and ν are the van Genuchten parameters.

The surface and subsurface are coupled using either continuity of head or a conductance concept, with exchanges between the two domains. The latter concept was used in this study and is shown below (Therrien et al., 2009):

$$q_e = \frac{k_r K_{zz}}{l_e}(\psi - d_0) \qquad (6)$$

where q_e is the exchange flux between the surface and subsurface domain [LT^{-1}]; K_{zz} is the vertical saturated hydraulic conductivity [LT^{-1}]; and l_e is the coupling length [L].

All of the equations above are solved simultaneously at each time step utilising either a finite difference, control volume finite difference or finite element approach (Therrien et al., 2009). For this study, the control volume finite difference method is used, due to its quick implementation on regular model grids and superior mass conservation (Partington et al., 2009).

A 3-D HGS model of the tilted V-catchment (Section 3.1) was developed in order to obtain the required simulated streamflow and baseflow. As shown in Fig. 3, the catchment is symmetrical. As a result, all simulations were conducted for only half of the catchment, as shown in Fig. 5. The simulated stream channel, which extends in the y direction, is 10m wide. In the x direction, perpendicular to the stream channel, the grid spacing is 50m from x=0-2000m and 10m from 2000-2010m. The grid spacing along the y axis is 50m. Therefore, the domain has 42 cells in the x direction and 61 cells in the y direction. In the z direction, there are 21 layers, with a discretisation of 0.5m for the first 10m below the surface and a single layer below this, with its thickness varying between 10 and 80m. Therefore, the maximum saturated thickness of the whole catchment is 90m. A critical depth boundary condition was utilized at the downstream end of the channel (nodes (2000,0,0) and (2010,0,0)) to allocate the surface head at these nodes to be at critical depth (d_0). The discharge Q_0 per unit width at the critical depth boundary is then given by:

$$Q_0 = \sqrt{g d_0^3} \tag{7}$$

A no flow boundary condition was used for the bottom and lateral subsurface domain, meaning that water can only leave the catchment from the stream outlet (i.e. critical depth boundary). The surface friction was described using Manning’s roughness coefficients of 0.015 and 0.15 for the slope and channel, respectively, as was the case in Panday and Huyakorn (2004). The rill storage and obstruction storage heights for this model implementation were also set to quite small values of 0.001m and 0.0m, respectively, to reduce their effects on baseflow generation. The coupling length used was 1x10^{-6}m, providing near continuity of pressure at the surface/subsurface interface.

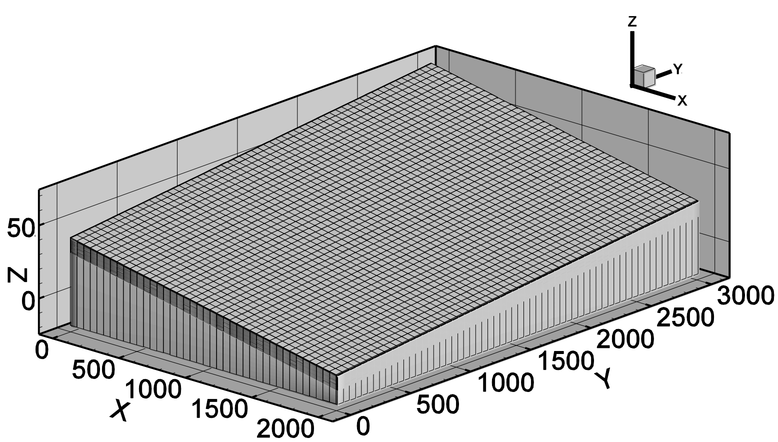

Fig. 5 Catchment model for case study (modified version of the V-catchment in Pandy and Huyakorn (2004))

The HGS model was used to simulate streamflow for catchments with different soil properties and the baseflow was calculated using the HMC method, details of which can be found in Partington et al. (2011). The two soil parameters that were varied include K_s and porosity (Table 1). For each soil type, each of the two parameters was varied over five values, the minimum, lower quartile, mean, upper quartile and maximum values of the ranges given in Table 1, while keeping the other soil parameter constant at its mean value. This resulted in 45 simulations in total; 9 for each of the five soil types in Table 1.

The simulations with different soil characteristics were conducted in three steps. Firstly, to determine steady initial conditions, a spatially and temporally uniform rainfall with a relatively high intensity (i.e. 10.8mm/hour) was applied to the catchment, with an initial water table parallel to the bottom of the channel across the whole catchment. This simulation was run for approximately one year until the total streamflow did not change with time, and was then allowed to drain under gravity in the next phase when the actual rainfall was applied.

Secondly, with the above initial conditions, the actual Adelaide rainfall record (see Section 3.1) was applied to the whole catchment and the model was run until a second equilibrium state based on the actual rainfall was reached, which required simulation periods between 2 and 35 years, depending on soil type. These simulations provided steady-state initial conditions for step three. It should be noted that, alternatively, initial conditions for different soil types can be obtained by directly applying the actual Adelaide rainfall to the catchment with a fully-saturated subsurface domain, and running the model until the catchment achieves a steady state. However, this method of deriving the initial condition takes much longer for some of the soil types considered, resulting in significantly diminished transient behavior caused by the inconsistent boundary or initial conditions. Finally, based on these equilibrium states for the actual rainfall record, the simulation was run for a further ten years in order to obtain the data used for assessing and improving the performance of the RDF. For all of the simulations, adaptive time stepping with a maximum time step of 1000s was used to ensure that the maximum time step is significantly less than hourly.

3.3. Digital Filter

In this study, the LH filter was used as the RDF. Although the LH filter has some limitations compared with other RDFs, such as the Chapman one-parameter algorithm (Chapman and Maxwell, 1996) and the Boughton two-parameter algorithm (Chapman, 1999) (e.g. it is unable to estimate baseflow when there is no direct runoff, as discussed by Chapman and Maxwell (1996)), it is used extensively in practice and has already been incorporated into a number of software tools, including BaseJumper (Murphy et al., 2009) and ABScan (Parker, 2006). The LH filter is a high-pass filter, which filters low frequency signals (i.e. baseflow) and transmits high-frequency input signals (i.e. quickflow). Consequently, baseflow has to be obtained by subtracting the filtered quickflow from the original streamflow. The corresponding equations are given by Nathan and McMahon (1990) as:

$$\begin{aligned} q_{f(i)} &= k q_{f(i-1)} + \frac{1+k}{2}(q_{(i)} - q_{(i-1)}) \quad for \quad q_{f(i)} \geq 0 \\ q_{b(i)} &= q_{(i)} - q_{f(i)} \end{aligned} \tag{8}$$

where i is the time step, in days [T]; $q_{(i)}$ is the original total streamflow at time step i, [LT^{-1}]; $q_{f(i)}$ and $q_{b(i)}$ are the filtered quickflow and corresponding baseflow at time step i, [LT^{-1}]; and k is the filter parameter, dimensionless, which is normally set in the range of 0.0-1.0.

Referring to equation (8), the initial condition is set as the total streamflow being equal to baseflow (i.e. $q_{b(1)} = q_{(1)}$). In order to better understand the impact of the values of the filter parameter on filter performance, it is useful to examine the outputs obtained from the LH filter for the extreme values of the filter parameter. If the LH filter parameter is set to its maximum value of 1.0, when $q_{(i)} > q_{(1)}$, the baseflow obtained using the LH filter at each time step is always equal to the first value of total streamflow ($q_{b(i)} = q_{(1)}$), even if there is a peak in the streamflow hydrograph. If $q_{(i)} \leq q_{(1)}$, the filtered baseflow is equal to the total streamflow ($q_{b(i)} = q_{(i)}$), due to the constrained condition that baseflow cannot exceed total streamflow or become negative. On the other hand, if the LH filter parameter is set to its minimum value of 0.0, for the rising limb of the total streamflow hydrograph, the baseflow obtained from the LH filter is attenuated by halving the sum of the values of the total streamflow at the current and previous time step ($q_{b(i)} = \dfrac{q_{(i-1)} + q_{(i)}}{2}$). As for the descending limb, the filtered baseflow is equal to the streamflow at the current time step ($q_{b(i)} = q_{(i)}$). Therefore, when the filter parameter is 0.0, the filtered baseflow hydrograph always has a peak right under the peak of the streamflow hydrograph. Baseflow hydrographs obtained from the LH filter with values of the filter parameter between 0.0 and 1.0 lie between the baseflow hydrographs derived using filter parameters of 0.0 and 1.0.

The filter can be passed forward and backward over a data set several times and the number of passes results in data smoothing and nullification of any phase distortion (Spongberg, 2000). Although some researchers have used a relatively large number of passes, such as Murphy et al. (2009), who implemented the LH filter with 9 passes across hourly data for eight case study catchments, most of the studies have used three passes (e.g. (Evans and Neal, 2005; Li et al., 2011; Spongberg, 2000; Tan et al., 2009b)), as suggested by Nathan and McMahon (1990). In this study, the filter was passed over the data three times in all of the analyses: forward, backward and then forward again. The time step ($i-1$) is replaced by ($i+1$) when conducting the "backward" pass, and after the first pass, $q_{(i)}$ is substituted by the computed baseflow calculated from the previous pass. During the calculation, if $q_{f(i)}$ is smaller than zero, the baseflow is equal to the current $q_{(i)}$.

The 45 simulated streamflow hydrographs obtained from the HGS model for the different combinations of soil properties were used as inputs to the LH filter in order to obtain the corresponding filtered baseflow. Two sets of 45 filtered baseflow hydrographs were obtained, one using optimal (calibrated) filter parameter values (see Section 3.4 for details) and one using a fixed filter parameter of 0.925, which is commonly used in the literature (Arnold and Allen, 1999; Murphy et al., 2009; Nathan and McMahon, 1990), in order to assess the potential benefits of obtaining calibrated filter parameter values.

3.4. Error Measure and Optimization Procedure

The dimensionless coefficient of efficiency (E_f) was used as the error measure for evaluating the performance of filters with different parameters and applied to catchments with different soil conditions. This is because it is one of the most commonly used error measures in hydrology and provides a trade-off between objectives that emphasize different aspects of hydrographs (Gupta and Kling, 2011; Gupta et al., 2009). However, it should be noted that because of the nature of the LH filter, constrains are placed on the variability of the resulting baseflow hydrograph. For example, as discussed previously, the timing of the peak of the baseflow hydrograph always coincides with the timing of the peak of the total streamflow hydrograph and whenever baseflow is larger than the total streamflow, baseflow is forced to be equal to the total streamflow, thereby capturing the recession limb of the baseflow hydrograph. As a result, the only variability is in the magnitude of the baseflow hydrograph, which is controlled by the LH filter parameter, as discussed above (i.e. smaller values of the filter parameter result in larger peaks and vice versa).

The equation of E_f was given by Nash and Sutcliffe (1970) as:

$$E_f = 1 - \left[\frac{\sum_{i=1}^{n} (Y_i^{obs} - Y_i^{sim})^2}{\sum_{i=1}^{n} (Y_i^{obs} - Y^{mean})^2} \right] \tag{9}$$

where Y_i^{obs} is the ith observation of the flow rate being evaluated [LT^{-1}], Y_i^{sim} is the ith simulated value of the flow rate being evaluated [LT^{-1}], Y^{mean} is the mean of the observed data for the flow rate being evaluated [LT^{-1}], i is the time step [T], and n is the total number of observations.

When using E_f to evaluate the performance of RDFs, the observed data in equation (9) are given by the simulated baseflow results obtained from the fully integrated SW/GW model (q_b^{sim}), while the baseflow results derived from the RDFs (q_b^{filter}) correspond to the simulated values. Based on benchmark values available from other studies (Herron and Croke, 2009; Moriasi et al., 2007; Nejadhashemi et al., 2007), RDF performance can be judged as 'perfect' when E_f=1.0, while E_f values between 0.5 and 1.0 correspond to 'good' filter performance; E_f values between 0.0 and 0.5 show 'acceptable' filter performance and 'unacceptable' filter performance is represented by negative values of E_f.

In order to estimate the uncertainty associated with estimates of the optimal LH filter parameters, the following linear estimate of uncertainty was used (Vugrin et al., 2005):

$$\left\{ k : \frac{S(k) - S(\hat{k})}{S(\hat{k})} \leq \frac{p}{n-p} F_{p,n-p}^{\alpha} \right\} \tag{10}$$

$$S(k) = \sum_{i=1}^{n} [q_{b(i)}^{filter}(k) - q_{b(i)}^{sim}]^2 \tag{11}$$

where $\hat{k}$ is the optimal LH filter parameter, obtained by minimizing the sum of squared errors between the baseflow obtained from the LH filter and that simulated using the HGS model (equation (11)); p is the number of parameters to be estimated, which is 1 in this case; n is the number of data points, which is 3650 days in this case; and $F^{\alpha}_{p,n-p}$ is the upper α percent point of the F-distribution, which was set to 0.05.

The optimization method used in order to obtain the optimal values of the filter parameters was the golden section search method (Press et al., 1992), as there was only one model parameter.

4. Results and Discussion

4.1. Relationship between Optimal Filter Parameters and Soil Properties

The optimal LH filter parameter values obtained for the different soil properties, as well as their linear estimates of uncertainty, are given in Table 2 and Fig. 6. As can be seen, the uncertainty estimates are very small, indicating that the optimal values of the filter parameters are well defined and that the results obtained can be treated with confidence. In addition, it can be seen that there is a distinct inverse relationship between K_s and optimal values of the LH filter parameter, which vary between 0.0025 and 0.997, while the optimal values of the LH filter parameter do not vary significantly for soils with different values of porosity. This can be explained by examining the relationship between soil properties and the resulting baseflow, as well as the relationship between the values of the LH filter parameter and filter performance (see below).

Relationship between soil properties and resulting baseflow

Soils with different values of porosity were found to have similar baseflow components. Although soils with larger porosity can store more subsurface water before they become saturated and also allow more groundwater to discharge into the stream, for a given value of K_s, their rate of change in storage was similar to that of soils with smaller porosity, resulting in similar baseflow components.

In contrast, for soils with a given porosity, soils with larger values of K_s resulted in larger baseflow components. This is because there is a positive relationship between K_s and the ease with which water can infiltrate into the soil, which means that larger K_s values enable water to infiltrate into the soil more easily, resulting in increased soil saturation and groundwater exfiltration. This can be seen from the simulated streamflow and baseflow obtained from the HGS models (Fig. 7). For catchments with sandy soil and mean values of K_s and porosity, most of the rain infiltrates into the ground, either percolating into the soil and staying in the catchment as groundwater or recharging the stream as baseflow. Consequently, compared with other soil types, the peak streamflow for sandy soils was smaller, with a high proportion of baseflow and a low proportion of quickflow (surface runoff). In contrast, for catchments with soil consisting of silt loam, rain cannot infiltrate easily, but is converted to direct runoff, rapidly feeding streamflow. Therefore, such catchments had streamflow with a higher peak, with almost no baseflow contribution.

Table 2 Optimal LH filter parameters and the linear estimates of uncertainty for sand, sandy loam, loam, loamy sand and silt loam with different soil properties

Soil Type	Min~Max	K_s & related optimal LH filter parameter				Porosity & related optimal LH filter parameter			
		K_s(m/s)	Filter Parameter	Lower Bound	Upper Bound	Porosity	Filter Parameter	Lower Bound	Upper Bound
Sand	Min	1.27E-06	0.997	0.9969	0.9976	0.261	0.415	0.4077	0.4241
	Lower Quartile	8.26E-05	0.787	0.7821	0.7937	0.31	0.465	0.458	0.4733
	Mean	1.60E-04	0.503	0.4956	0.5104	0.359	0.503	0.4956	0.5104
	Upper Quartile	5.65E-04	0.105	0.098	0.1142	0.409	0.537	0.5293	0.5474
	Max	9.66E-04	0.0025	0.0	0.01	0.4578	0.571	0.5635	0.5777
Sandy Loam	Min	5.01E-07	0.997	0.9969	0.9975	0.28	0.990	0.989	0.9907
	Lower Quartile	1.25E-05	0.997	0.9967	0.9982	0.346	0.991	0.9898	0.9916
	Mean	2.44E-05	0.992	0.9914	0.9938	0.412	0.992	0.9914	0.9938
	Upper Quartile	7.51E-05	0.837	0.833	0.8427	0.478	0.992	0.9913	0.9934
	Max	1.26E-04	0.612	0.605	0.6186	0.544	0.994	0.9929	0.995
Loam	Min	8.17E-06	0.997	0.9967	0.9978	0.29	0.983	0.9815	0.9836
	Lower Quartile	1.57E-05	0.997	0.9963	0.9979	0.422	0.986	0.9846	0.9864
	Mean	3.07E-05	0.987	0.9864	0.988	0.554	0.987	0.9864	0.988
	Upper Quartile	9.46E-05	0.719	0.7133	0.7257	0.686	0.988	0.9873	0.9891
	Max	1.58E-04	0.458	0.4501	0.4679	0.818	0.990	0.9885	0.9906
Loamy Sand	Min	1.10E-05	0.997	0.9966	0.9978	0.341	0.970	0.969	0.9713
	Lower Quartile	2.55E-05	0.996	0.9948	0.9967	0.398	0.973	0.9715	0.9738
	Mean	3.99E-05	0.974	0.9732	0.9753	0.455	0.974	0.9732	0.9753
	Upper Quartile	1.12E-04	0.665	0.6582	0.6713	0.512	0.976	0.975	0.9769
	Max	1.84E-04	0.438	0.4304	0.4477	0.569	0.978	0.9772	0.9794
Silt Loam	Min	1.51E-07	0.997	0.9968	0.9974	0.35	0.997	0.9968	0.9977
	Lower Quartile	1.58E-06	0.997	0.9969	0.9976	0.425	0.997	0.9968	0.9977
	Mean	3.01E-06	0.997	0.9968	0.9977	0.5	0.997	0.9968	0.9977
	Upper Quartile	8.41E-06	0.997	0.9967	0.9979	0.575	0.997	0.9968	0.9977
	Max	1.38E-05	0.997	0.9967	0.9982	0.65	0.997	0.997	0.9973

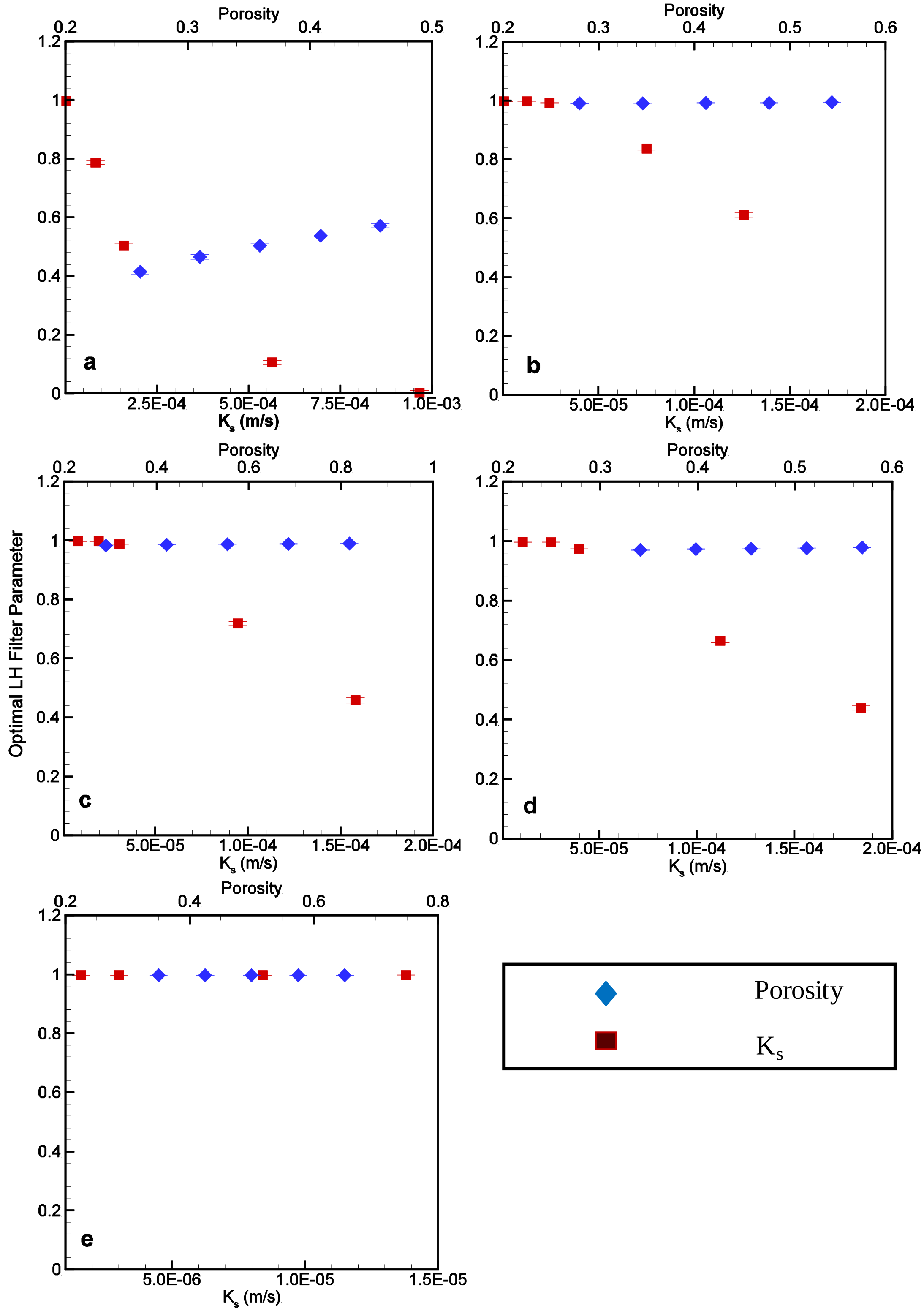
Porosity
Optimal LH Filter Parameter
K_s (m/s)
a
b
c
d
e
Porosity
K_s

Fig. 6. Values of the optimal LH filter parameter with the error bars obtained from the linear estimates of uncertainty for sand (a), sandy loam (b), loam (c), loamy sand (d) and silt loam (e) with different soil properties

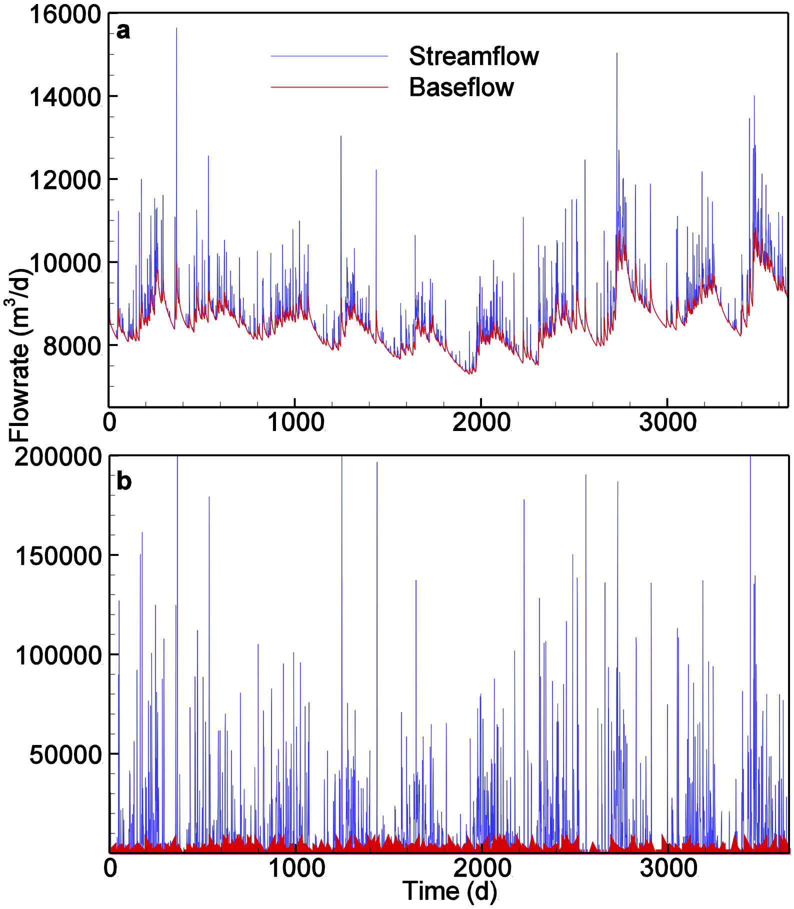

Fig. 7. Simulated streamflow and baseflow for catchments with sand (a) and silt loam (b) with their mean values of K_s and porosity

This difference in the streamflow behaviour for the two different soil types can also be seen clearly by examining the corresponding flow duration curves, which are an estimate of the percentage of time a particular streamflow was equaled or exceeded, and therefore provide a graphical representation of the variability associated with streamflow (Vogel and Fennessey, 1994). As can be seen from Fig. 8, the flow duration curve for the catchment with a sandy soil is very flat, indicating that streamflow is almost constant over time, which is representative of a stream that is fed primarily by baseflow. In contrast, the flow duration curve for the catchment consisting of silt loam indicates that flows are highly variable, with higher peak flows, but extended periods with little or no flow, which is indicative of a catchment that is dominated by surface flow.

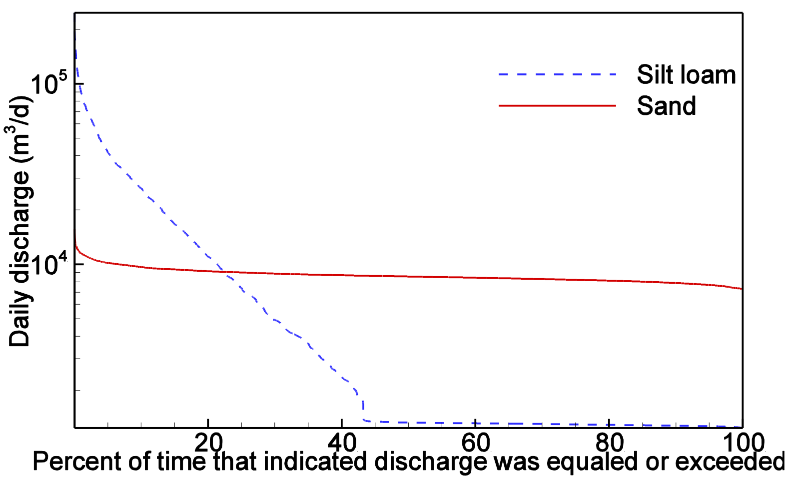

Fig. 8. Flow duration curves for catchments with sand and silt loam with their mean values of K_s and porosity

Relationship between the values of the LH filter parameter and filter performance

As discussed above, larger values of K_s result in larger baseflow and vice versa, and as discussed in Section 3.3 and shown in Fig. 9, for a catchment with sandy soil, smaller values of the LH filter parameter result in larger baseflow contributions and vice versa. Consequently, there exists an inverse relationship between K_s and the optimal LH filter parameter values, as shown in Fig. 6.

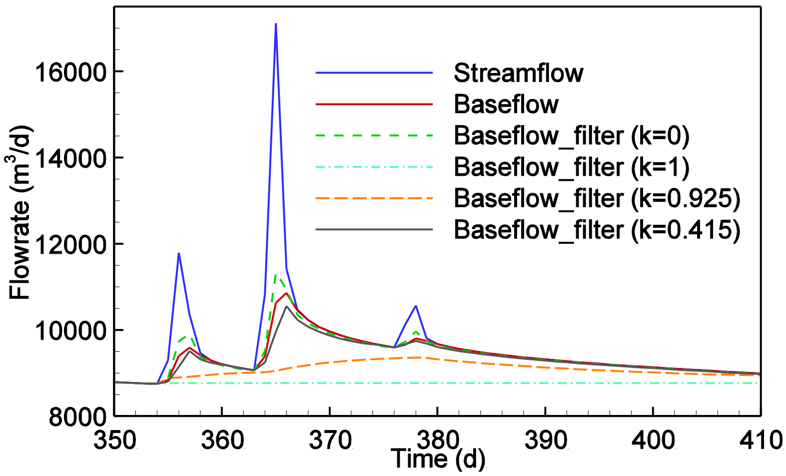

Fig. 9. Impact of different values of LH filter parameter on baseflow for catchment with sand with minimum porosity

To further confirm the inverse relationship between K_s and the optimal value of the LH filter parameter, five additional simulations (i.e. generation of simulated streamflow and baseflow using HGS, optimization of the LH filter parameter and the determination of filtered baseflow) were conducted with K_s values between the mean and upper quartile values of K_s for sand. The results obtained for all of the simulations conducted are shown in Fig. 10, including the linear estimates of uncertainty, which are very small, indicating that the results obtained can be treated with confidence. As can be seen, the additional results confirm the strong inverse relationship between the optimal value of the LH filter parameters and K_s, regardless of soil type, which is as expected, based on the discussion of the impact of K_s on baseflow and the way different filter parameter values affect the output from the LH filter given above. However, as can be seen from Fig. 10, the optimal values of the LH filter parameter are almost constant very close to their maximum value of 1.0 for soils with small values of K_s, suggesting that for small values of K_s, baseflow estimates obtained using the LH filter might be inaccurate, as baseflow decreases with decreasing values of K_s, while the baseflow hydrographs obtained using the LH filter remain constant (also see Section 4.2). In addition, it can be seen that the optimal values of the filter parameter can be significantly different from the value of 0.925 most commonly used in the literature (Murphy et al., 2009; Nathan and McMahon, 1990).

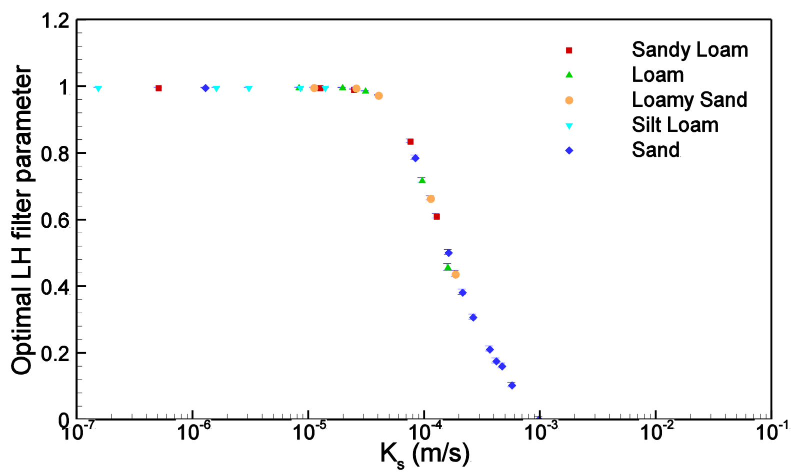

Fig. 10. Relationship between the optimal LH filter parameter and K_s with the error bars obtained from the linear estimates of uncertainty for different soil properties

4.2. Relationship between Filter Performance and Soil Properties

Since K_s has the most significant impact on baseflow among the different soil parameters investigated, only baseflow results obtained for soils with different values of K_s are discussed in this section. The E_f values between the baseflow obtained using the LH filter with optimal filter parameters and the simulated baseflow from HGS are summarized in Table 3. As can be seen, in most cases, the filtered baseflow is similar to that obtained from the HGS model, especially for soils with larger values of K_s. For example, for sand with the maximum K_s value, the filtered baseflow obtained with the optimal filter parameter of 0.0025 is almost identical to the simulated baseflow obtained using HGS (Fig. 11), with an E_f of 0.9998 (Table 3). In this case, the high K_s value results in most of the rain infiltrating into the ground and becoming groundwater, leading to increased exfiltration to the stream. As a result, surface runoff from the catchment is quite low, but the baseflow component of the streamflow is quite high. The same results can be observed from the flow duration curve for sand with maximum K_s (Fig. 12). The flat slope of this curve throughout denotes the characteristics of a perennial stream, with continuous and significant baseflow discharge. Consequently, a very low value of the LH filter parameter is optimal, as discussed previously. Similar results were obtained for soils with K_s values greater than 2.44E-05m/s, provided the optimal LH filter parameter was used. Based on the results obtained, it is suggested that the baseflow obtained using the LH filter can provide a good approximation to the actual baseflow for perennial streams, in catchments with soils with relatively large values of K_s, as long as an appropriate value of the filter parameter is used.

Table 3 Comparison of LH filter performance for the case where the optimal filter parameter was used and a filter parameter of 0.925 was used for sand, sandy loam, loam, loamy sand and silt loam with different K_s

Soil type		K_s (m/s)	E_f between simulated baseflow and that obtained using LH filter with the optimal filter parameter	E_f between simulated baseflow and that obtained using LH filter with a filter parameter of 0.925
Sand	Min	1.27E-06	-2.266	-19.613

	Lower quartile	8.26E-05	0.960	0.900
	Mean	1.60E-04	0.989	0.903
	Upper quartile	5.65E-04	0.999	0.969
	Max	9.66E-04	0.9998	0.976
Sandy loam	Min	5.01E-07	-10.29	-73.56
	Lower quartile	1.25E-05	-0.044	-1.945
	Mean	2.44E-05	0.290	-0.679
	Upper quartile	7.51E-05	0.965	0.946
	Max	1.26E-04	0.981	0.900
Loam	Min	8.17E-06	-0.135	-2.704
	Lower quartile	1.57E-05	0.010	-1.613
	Mean	3.07E-05	0.517	-0.078
	Upper quartile	9.46E-05	0.958	0.888
	Max	1.58E-04	0.986	0.884
Loamy sand	Min	1.10E-05	-0.083	-2.136
	Lower quartile	2.55E-05	0.137	-1.125
	Mean	3.99E-05	0.825	0.698
	Upper quartile	1.12E-04	0.981	0.924
	Max	1.84E-04	0.991	0.906
Silt loam	Min	1.51E-07	-76.85	-489.41
	Lower quartile	1.58E-06	-1.603	-14.84
	Mean	3.01E-06	-0.589	-6.966
	Upper quartile	8.41E-06	-0.130	-2.651
	Max	1.38E-05	-0.029	-1.813

The performance of the LH filter is not as good for soils with small values of K_s, with small and even negative values of E_f (Table 3). For example, for silt loam with the minimum K_s value, the baseflow obtained using the filter with the optimal value of the filter parameter is much larger than the simulated baseflow obtained using HGS at almost all time steps (Fig. 11), resulting in an E_f of -76.85. The reason for this is that K_s determines how much water infiltrates into the ground and how easily water moves through the subsurface of the catchment. Therefore, for a catchment with low K_s and high intensity rainfall, infiltration is low, which results in the generation of more surface runoff and the formation of sharp peaks in observed streamflow (Fig. 11). Consequently, the simulated baseflow is quite small, with small fluctuations around the mean value at all time steps. This can be seen from the flow duration curve for silt loam with minimum K_s (Fig. 12). This curve has a reasonably steep slope throughout, which intercepts the x-axis at around 53% of time, indicating that all of the discharges are less than or equal to the discharge that occurs 53% of the time. This flow duration curve is indicative of a highly variable ephemeral stream, the flow of which is largely from direct runoff with very small contributions from baseflow. Streams like this may cease to flow for relatively long periods without rainfall events. However, as discussed previously, the baseflow obtained using the LH filter is based solely on streamflow and the value of the filter parameter, so that the variations in filtered baseflow follow the sharp variations in streamflow, resulting in an over-prediction of baseflow whenever the filter parameter is between 0.0 and 1.0. Therefore, the LH filter does not appear to be suitable for catchments with K_s values smaller than 1.38E-05m/s that result in variable ephemeral streams with low baseflow contribution, even when the optimal filter parameter is used. This is an agreement with the discussion of Fig. 10 in Section 4.1. It should be noted that, in practice, if the catchment has very little baseflow, there is generally no need to estimate it. However, the simulations for low baseflow contribution catchments (e.g. silt loam with minimum K_s) are shown here in order to illustrate the sorts of features, such as soil properties, that cause the catchment to have little baseflow contribution.

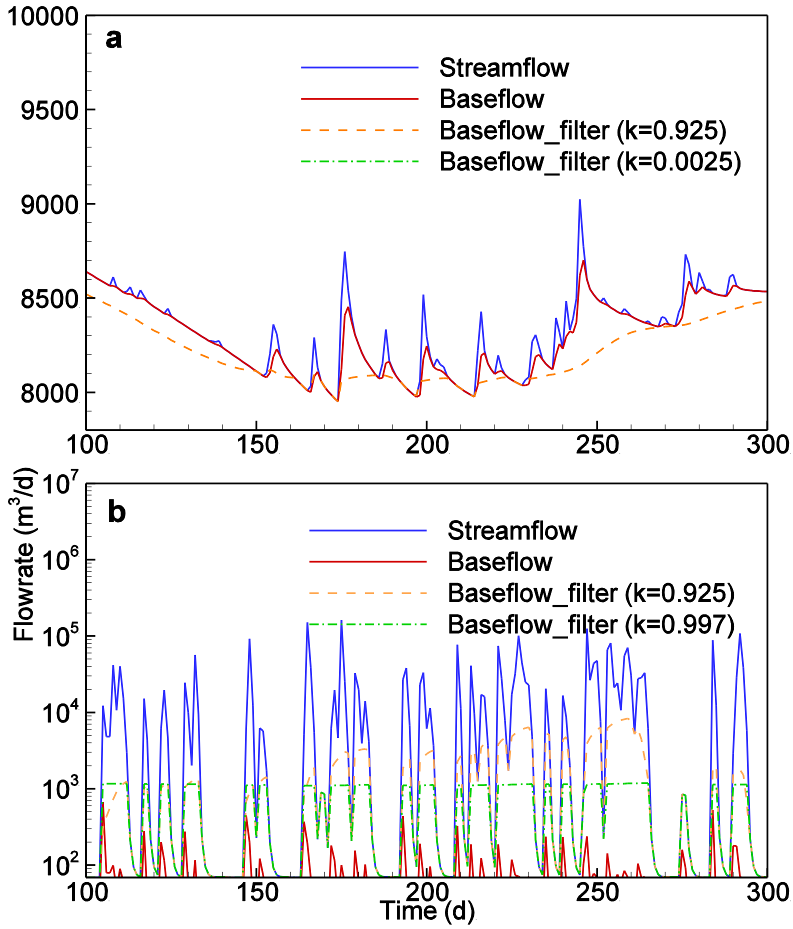

Fig. 11. Comparison of baseflow calculated from the HGS model simulation and the LH filter with two different values of the filter parameter for sand with maximum K_s (a) and silt loam with minimum K_s (b)

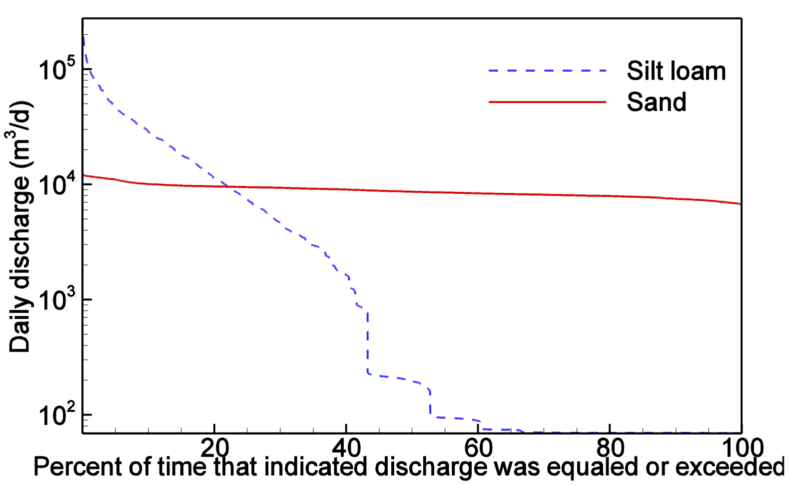

Fig. 12. Flow duration curves for catchments with sand with maximum K_s, and silt loam with minimum K_s

The performance of the LH filter with the most commonly used filter parameter of 0.925 is also shown in Table 3 and Fig. 11. As can be seen, by obtaining optimal values of the LH filter parameter for different soil properties, the performance of the LH filter can be improved significantly in certain situations. This is to be expected, given that the optimal values of the filter parameter for soils with different properties span such a large range, as discussed above. The results obtained indicate that the performance of the LH filter with a filter parameter of 0.925 is not adequate for most of the catchments with small values of K_s, but acceptable for catchments with K_s values greater than 3.99E-05m/s, with E_f values greater than 0.698. However, the range of soil types over which the LH filter performs well can be extended by using the filter parameter that is most appropriate for the soil conditions.

The results presented in this paper have utilized the simulations from the fully integrated SW/GW model as though they are the 'true' values. The results derived using this framework for this hypothetical case study illustrate the impacts of catchment soil properties on RDF parameters, and provide a clearer understanding that among catchment soil properties, K_s is likely to play a key role in determining the appropriate values of optimal filter parameters for catchments with different physical properties. Physical processes in real catchments are more complicated than those represented in the hypothetical case study, due to catchment heterogeneity, macropores, and vegetation; however, the dominant physical processes are captured by the fully integrated SW/GW model, which clearly identifies the need for a variable filter parameter, and to carefully consider the application of digital filtering approaches to determining baseflow.

5. Summary and Conclusions

In this study, a generic framework for assessing and improving currently used RDFs for quantifying baseflow has been developed. This framework provides a procedure that enables research studies to be conducted in order to test the accuracy and improve the performance of various baseflow filter methods. The framework makes use of fully integrated surface water and groundwater (SW/GW) models to obtain estimates of streamflow and baseflow for catchments with different properties (e.g. soil types and rainfall patterns). A recursive digital filter (RDF) is then applied to the simulated streamflow to estimate baseflow, which can be compared with the simulated baseflow obtained from the fully integrated SW/GW model in order to assess filter performance. Filter performance can be improved by adjusting the filter parameter(s) until the best match between the filtered baseflow hydrograph and the simulated baseflow hydrograph from the fully integrated SW/GW model is obtained. If a sufficient number of studies of this nature are conducted (i.e. using different RDFs, different fully integrated SW/GW models, different catchment hydrogeological properties, etc.), general guidelines for the applicability and improvement of RDFs can be developed.

In order to demonstrate the usefulness of the proposed framework, it was applied to a commonly used hypothetical case study. A fully integrated SW/GW model of a hypothetical catchment was developed using HGS, which was used to generate streamflow and baseflow hydrographs for 45 different soil properties. The generated streamflow hydrographs were used as inputs to the LH filter, which was applied using two sets of filter parameters; a constant value of 0.925, which is the value most commonly used in the literature, and values that were calibrated in order to minimize the difference between the baseflow hydrograph obtained using the LH filter and that obtained using the HGS model for each of the soil types. The results obtained show that the optimal value of the LH filter parameter is sensitive to the saturated hydraulic conductivity (K_s), and should therefore be adjusted accordingly, thus better reflecting the actual physical processes producing the baseflow. The results obtained also show that the baseflow obtained using the LH filter can represent the baseflow simulated using the HGS model reasonably well for catchments with relatively large K_s. However, for catchments with small values of K_s, the LH filter does not appear to be suitable. Furthermore, when a fixed filter parameter of 0.925 is used, the range of soil properties over which the LH filter is applicable is reduced significantly.

It should be noted that the generalisability of the results is restricted by the range of factors considered in the analysis. For example, consideration of the impact of vegetation and thus transpiration is likely to affect seasonal and longer term trends in baseflow as a result of vegetation growth, which could result in significantly more complex interactions (D'Odorico et al., 2005; Guttal and Jayaprakash, 2007, 2009). One must also be aware of the fact that no calibration-evaluation was undertaken to independently assess the calibrated LH filter parameters. Also, it should be noted that repetition of the analysis conducted in this paper with different climate records would possibly lead to other optimal LH filter parameters for the same soil type. Consequently, this should be the focus of future studies. Furthermore, it should be noted that the optimal values of the LH filter parameter are likely to be influenced by a number of other factors, such as catchment size, slope and aspect ratio, streamflow routing, soil heterogeneity, maximum saturated thickness and depth to water table. The impact of these factors on the optimal LH filter parameter should be investigated in future studies.

6. Acknowledgements

This research was supported by the Chinese Scholarship Council (CSC) and the University of Adelaide. The authors also gratefully thank Dr. Philip Brunner, Dr. Tim Peterson and the other anonymous reviewer for their detailed comments, which have greatly improved the quality of the paper.

7. References

Arnold, J.G., Allen, P.M., 1999. Automated Methods for Estimating Baseflow and Ground water Recharge from Streamflow Records. Journal of the American Water Resources Association 35(2) 411-424.

Arnold, J.G., Allen, P.M., Muttiah, R., Bernhardt, G., 1995. Automated Baseflow Separation and Recession Analysis Techniques. Ground Water 33(6) 1010-1018.

Bako, M.D., Hunt, D.N., 1988. Derivation of baseflow recession constant using computer and numerical analysis. Hydrological Sciences 33(4) 357-367.

Banks, E.W., Brunner, P., Simmons, C.T., 2011. Vegetation controls on variably saturated processes between surface water and groundwater and their impact on the state of connection. Water Resources Research 47(11) W11517.

Brookfield, A.E., Sudicky, E.A., Park, Y.-J., Jr., B.C., 2009. Thermal transport modelling in a fully integrated surface/subsurface framework. Hydrological Processes 23(15) 2150-2164.

Brunner, P., Cook, P.G., Simmons, C.T., 2009. Hydrogeologic controls on disconnection between surface water and groundwater. Water Resources Research 45(1) W01422.

Chapman, T., 1999. A comparison of algorithms for stream flow recession and baseflow separation. Hydrological Processes 13(5) 701-714.

Chapman, T.G., Maxwell, A.I., 1996. Baseflow separation-Comparison of numerical methods with tracer experiments, Proceedings of the 23rd hydrology and water resources symposium: Hobart Australia.

D'Odorico, P., Laio, F., Ridolfi, L., 2005. Noise-induced stability in dryland plant ecosystems, Proceedings of the National Academy of Sciences of the United States of Amrica, pp. 10819-10822.

DiGiammarco, P., Todini, E., P., L., 1996. A conservative finite elements approach to overland flow: The control volume finite element formulation. Journal of Hydrology 175 267-291.

Doble, R., Brunner, P., McCallum, J., Cook, P.G., 2012. An Analysis of River Bank Slope and Unsaturated Flow Effects on Bank Storage. Ground Water 50(1) 77-86.

Dukic, V., 2006. Modeling of base flow of the Basin of Kloubara River in Serbia. Journal of Hydrology 327(1-2) 1-12.

Eckhardt, K., 2005. How to construct recursive digital filters for baseflow separation. Hydrological Processes 19(2) 507-515.

Eckhardt, K., 2008. A Comparison of Baseflow indices, which were calculated with seven different baseflow separation methods. Journal of Hydrology 352(1-2) 168-173.

Evans, R., Neal, B., 2005. Baseflow analysis as a tool for groundwater-surface water interaction assessment, International Water Conference: Auckland, New Zealand.

Ferket, B.V.A., Samain, B., Pauwels, V.R.N., 2010. Internal validation of conceptual rainfall–runoff models using baseflow separation. Journal of Hydrology 381 158-173.

Furey, P.R., Gupta, V.K., 2001. A physically based filter for separating base flow from streamflow time series. Water Resources Research 37(11) 2709-2722.

Furman, A., 2008. Modelling coupled surface-subsurface flow processes: a review. Vadose Zone Journal 7(2) 741-756.

Gibbs, M.S., Maier, H.R., Dandy, G.C., 2012. A generic framework for regression regionalization in ungauged catchments. Environmental Modelling & Software 27–28(0) 1-14.

Gilfedder, M., Walker, G.R., Dawes, W.R., Stenson, M.P., 2009. Prioritisation approach for estimating the biophysical impacts of land-use change on stream flow and salt export at a catchment scale. Environmental Modelling & Software 24(2) 262-269.

Gupta, H.V., Kling, H., 2011. On typical range, sensitivity, and normalization of Mean Squared Error and Nash-Sutcliffe Efficiency type metrics. Water Resour. Res. 47(10) W10601.

Gupta, H.V., Kling, H., Yilmaz, K.K., Martinez, G.F., 2009. Decomposition of the mean squared error and NSE performance criteria: Implications for improving hydrological modelling. Journal of Hydrology 377 80-91.

Guttal, V., Jayaprakash, C., 2007. Impact of noise on bistable ecological systems. Ecological Modelling 201(3–4) 420-428.

Guttal, V., Jayaprakash, C., 2009. Spatial variance and spatial skewness: leading indicators of regime shifts in spatial ecological systems. Theoretical Ecology 2(1) 3-12.

Hall, F.R., 1968. Base-Flow Recession-A Review. Water Resour. Res. 4.

Herron, N., Croke, B., 2009. Including the influence of groundwater exchanges in a lumped rainfall-runoff model. Mathematics and Computers in Simulation 79(9) 2689-2700.

HydroGeoLogic, 2000. MODHMS: a comprehensive MODFLOW-based hydrologic modeling system., Version 1.1. Code Documentation and User's Guide: HydroGeoLogic Inc., Herndon, VA, USA.

Jones, J.P., Sudicky, E.A., Brookfield, A.E., Park, Y.-J., 2006. An assessment of the tracer-based approach to quantifying groundwater contributions to streamflow. Water Resources Research 42(2) W02407.

Khan, S., Yufeng, L., Ahmad, A., 2009. Analysing complex behaviour of hydrological systems through a system dynamics approach. Environmental Modelling & Software 24(12) 1363-1372.

Kollet, S.J., Maxwell, R.M., 2006. Integrated surface-groundwater flow modeling: A free-surface overland flow boundary condition in a parallel groundwater flow model. Advances in Water Resources 29(7) 945-958.

Li, L., Maier, H.R., Lambert, M.F., Simmons, C.T., Partington, D., 2011. Sensitivity of optimal baseflow filter parameters to catchment soil characteristics, Proceedings of the 34th IAHR World COngress: Brisbane, Australia, pp. 1643-4650.

Linsley, R.K., Kohler, M.A., Paulhus, J.L.H., Wallace, J.S., 1988. Hydrology for Engineers. McGraw-Hill Book Co., Singapore.

Lyne, V., Hollick, M., 1979. Stochastic Time-Variable Rainfall-Runoff Modelling, I.E. Aust. Natl. Conf. Publ. Inst. of Eng.: Canberra, Australia, pp. 89-93.

Marsh, T.J., Hannaford, J., 2008. Hydrological data UK. UK Hydrometric Register. Center for Ecology & Hydrology: Wallingford, p. 210.

Mau, D.P., Winter, T.C., 1997. Estimating Groundwater Recharge from Streamflow Hydrographs for a Small Mountain Watershed in a Temperate Humid Climate. Groundwater 35(2) 291-304.

McCallum, J.L., Cook, P.G., Brunner, P., Berhane, D., 2010. Solute dynamics during bank storage flows and implications for chemical base flow separation. Water Resour. Res. 46(7) W07541.

Moriasi, D.N., Arnold, J.G., Liew, M.W.V., Bingner, R.L., Harmel, R.D., Veith, T.L., 2007. Model evaluation guidelines for systematic quantification of accuracy in watershed simulations. American Society of Agriculture and Biological Engineers 50(3) 885-900.

Murphy, R., Graszkiewicz, Z., Hill, P., Neal, B., Nathan, R.J., Ladson, T., 2009. Project 7: Baseflow for catchment simulation (Phase 1- Selection of baseflow separation approach). Australian Rainfall and Runoff Technical Committee: Australia.

Nash, J.E., Sutcliffe, J.V., 1970. River flow forecasting through conceptual models: Part 1. A discussion of principles. Journal of Hydrology 10(3) 282-290.

Nathan, R.J., McMahon, T.A., 1990. Evaluation of Automated Techniques for Base Flow and Recession Analysis. Water Resources Research 26(7) 1465-1473.

Nejadhashemi, A.P., Shirmohammadi, A., Montas, H.J., 2003. Evaluation of Streamflow Partitioning Methods, ASAE Annual International Meeting. American Society of Agricultural Engineers: Las Vegas, Nevada, USA, p. 13.

Nejadhashemi, A.P., Shirmohammadi, A., Montas, H.J., Sheridan, J.M., Bosch, D.D., 2007. Analysis of watershed physical and hydrological effects on baseflow separation, 2007 ASABE Annual International Meeting, Technical Papers. American Society of Agricultural and Biological Engineers: Minneapolis, MN, United states.

Nejadhashemi, A.P., Shirmohammadi, A., Sheridan, J.M., Montas, H.J., Mankin, K.R., 2009. Case Study: Evaluation of Streamflow Partitioning Methods. Journal of Irrigation & Drainage Engineering 135(6) 791-801.

Panday, S., Huyakorn, P.S., 2004. A fully coupled physically-based spatially-distributed model for evaluating surface/subsurface flow. Advances in Water Resources 27(4) 361-382.

Parker, G., 2006. Automated Baseflow Separation for Canadian Datasets (ABSCAN): User's Manual, Thinknew Analytics: Ottawa, Canada.

Partington, D., Brunner, P., Simmons, C.T., Therrien, R., Werner, A.D., Dandy, G.C., Maier, H.R., 2011. A hydraulic mixing-cell method to quantify the groundwater component of streamflow within spatially distributed fully integrated surface water-groundwater flow models. Environmental Modelling & Software 26(7) 886-898.

Partington, D., Brunner, P., Simmons, C.T., Werner, A.D., Therrien, R., Maier, H.R., Dandy, G.C., 2012. Evaluation of outputs from automated baseflow separation methods against simulated baseflow from a physically based, surface water-groundwater flow model. Journal of Hydrology 458–459 28-39.

Partington, D., Werner, A.D., Brunner, P., Simmons, C.T., Dandy, G.C., Maier, H.R., 2009. Using a fully coupled surface water-groundwater model to quantify streamflow components, World IMACS/MODSIM Congress: Cairns, Australia.

Press, W.H., Teukolsky, S.A., Vetterling, W.T., Flannery, B.P., 1992. Numerical recipes in FORTRAN 77: the art of scientific computing. Cambridge University Press, Cambridge.

Puhlmann, H., Von Wilpert, K., Lukes, M., Droge, W., 2009. Multistep outflow experiments to derive a soil hydraulic database for forest soils. European Journal of Soil Science 60(5) 792-806.

Ravazzani, G., Rametta, D., Mancini, M., 2011. Macroscopic cellular automata for groundwater modelling: A first approach. Environmental Modelling & Software 26(5) 634-643.

Schwartz, F.W., Sudicky, E.A., Mclaren, R.G., Park, Y.-J., Huber, M., Apted, M., 2010. Ambiguous hydaulic head and 14C activities in transient regional flow. Ground Water 48(3) 366-379.

Sloto, R.A., Crouse, M.Y., 1996. HYSEP: A Computer Program for Streamflow Hydrograph Separation and Analysis. U.S. Geological Survey: Pennsylvania.

Spongberg, M.E., 2000. Spectral analysis of base flow separation with digital filters. Water Resour. Res. 36(3) 745-752.

Sulis, M., Meyerhoff, S.B., Paniconi, C., Maxwell, R.M., Putti, M., Kollet, S.J., 2010. A comparison of two physics-based numerical models for simulating surface water-groundwater interactions. Advances in Water Resources 33(4) 456-467.

Tan, S.B.K., Lo, E.Y.-M., Shuy, E.B., Chua, L.H.C., Lim, W.H., 2009a. Generation of Total Runoff Hydrographs Using a Method Derived from a Digital Filter Algorithm. Journal of Hydrologic Engineering 14(1) 101-106.

Tan, S.B.K., Lo, E.Y.-M., Shuy, E.B., Chua, L.H.C., Lim, W.H., 2009b. Hydrograph Separation and Development of Empirical Relationships Using Single-Parameter Digital Filters. Journal of Hydrologic Engineering 14(3) 271-279.

Therrien, R., McLaren, R.G., Sudicky, E.A., Panday, S.M., 2009. HydroGeoSphere: A Three-dimensional Numerical Model Describing Fully-integrated Subsurface and Surface Flow and Solute Transport: Waterloo.

Therrien, R., Sudicky, E.A., 1996. Three-dimensional analysis of variably-saturated flow and solute transport in discretely-fractured porous media. Journal of Contaminant Hydrology 23(1-2) 1-44.

Van Genuchten, M.T., 1980. A closed-form Equation for Predicting the Hydraulic Conductivity of Unsaturated Soils. Soil Science Society of America Journal 44(5) 892-898.

VanderKwaak, J.E., Loague, K., 2001. Hydrologic-response simulations for the R-5 catchment with a comprehensive physics-based model. Water Resources Research 37(4) 999-1013.

Vogel, R.M., Fennessey, N.M., 1994. Flow-duration curves--New interpretation and confinence intervals. Journal of Water Resources Planning and Management 120(4) 485-504.

Vugrin, K.W., Swiler, L.P., Roberts, R.M., Stucky-Mack, N.J., Sullivan, S.P., 2005. Confidence Region Estimation Techniques for Nonlinear Regression: Three Case Studies. Sandia National Laboratories: New Mexico and California, p. 31.

Cover Letter

Li Li
School of Civil, Environmental and Mining Engineering
The University of Adelaide
Adelaide, South Australia
AUSTRALIA 5005

Editorial Office

Environmental Modelling & Software

Adelaide, 01 November 2012

Revisions of a manuscript by Li et al.

Dear Professor Jakeman

We are pleased to submit our revised manuscript entitled "Framework for Assessing and Improving the Performance of Recursive Digital Filters for Baseflow Estimation with Application to the Lyne and Hollick Filter" by Li Li, Holger R. Maier, Martin F. Lambert, Craig T. Simmons and Daniel J. Partington for consideration of publication in Environmental Modelling & Software.

All of the comments were addressed carefully. Please find a detailed description of the changes in 'Response to the Reviewers' attached to this submission.

On behalf of all co-authors, I would like to thank you very much for the very efficient handling of the manuscript, as well as for the very thoughtful and insightful reviews that have lead to a superior manuscript. We are looking forward to hearing from you.

Yours sincerely,

Li Li

Figure(s)

Figure 1

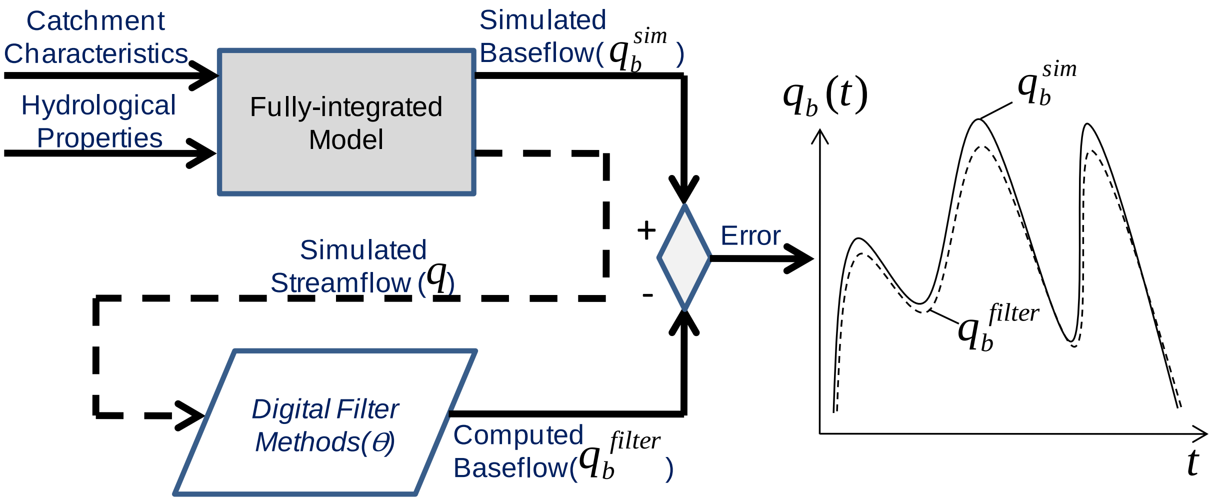

Schematic description of the framework for assessing the performance of RDFs for baseflow estimation

Figure(s)

Figure 2

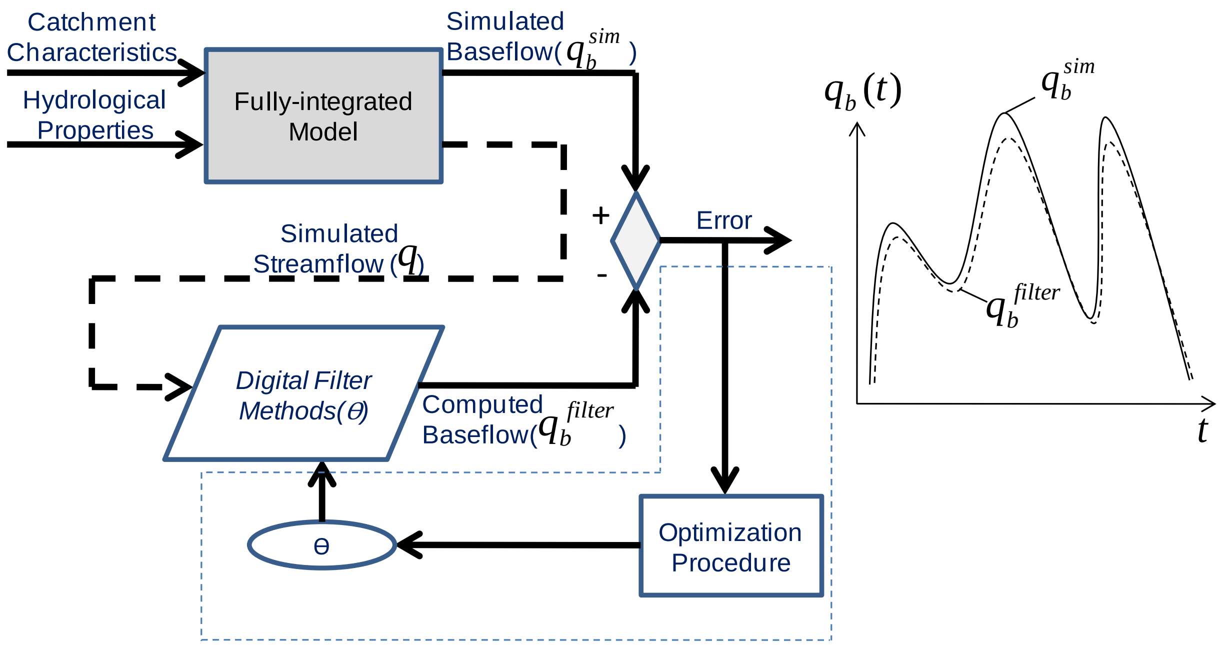

Schematic description of the framework for improving the performance of RDFs for baseflow estimation

Figure(s)

Figure 3

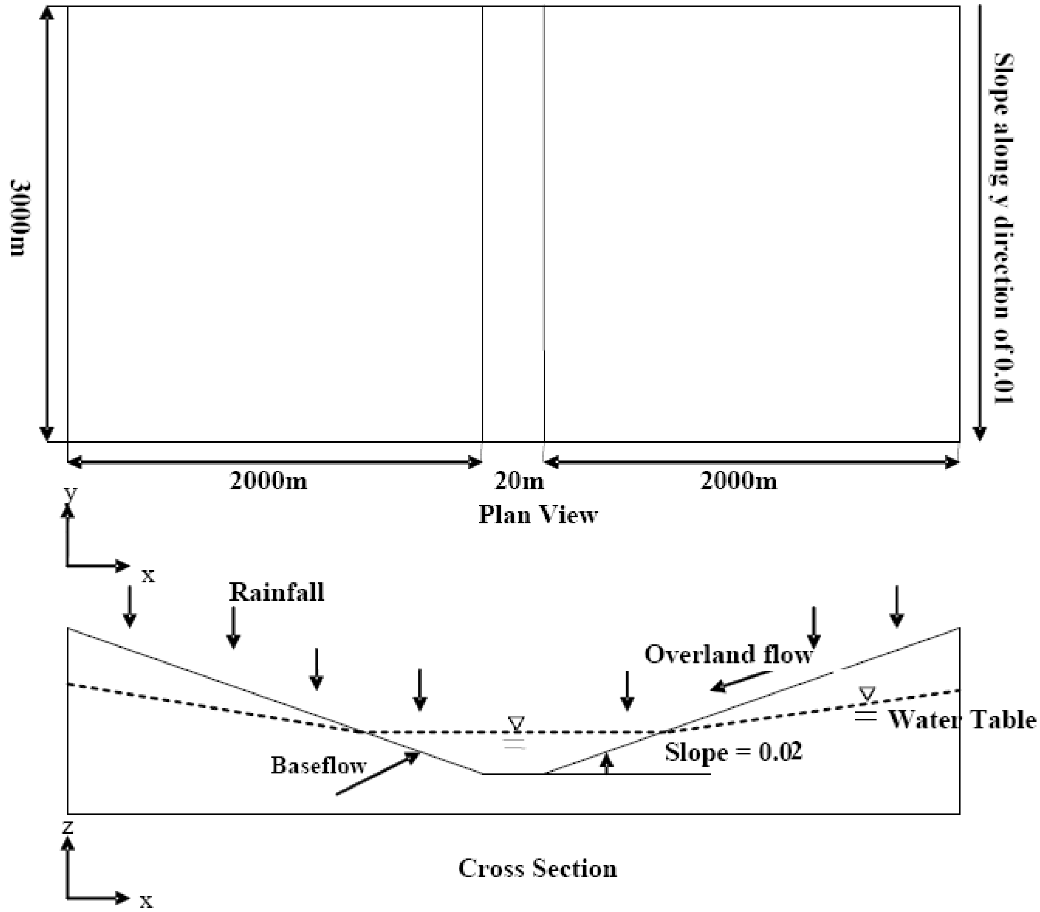

Schematic Representation of Tilted V-Catchment Flow Problem (Refer to Panday and Huyakorn (2004))

Figure(s)

Figure 4

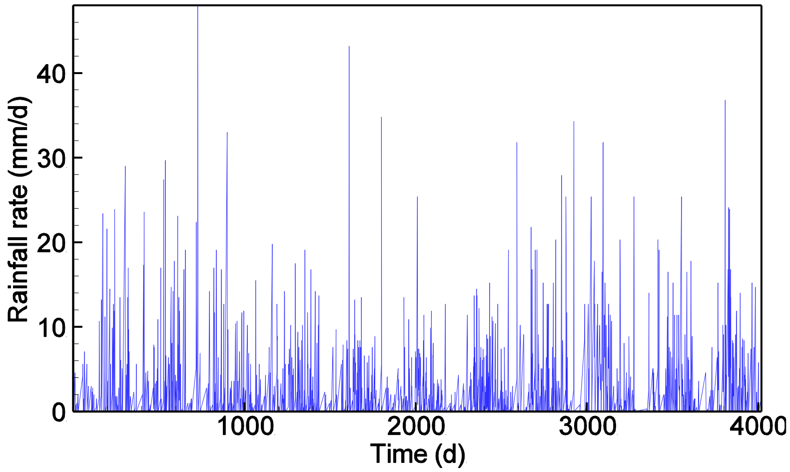

10 year daily rainfall data for Adelaide, South Australia, gauge number 23000

Figure(s)

Figure 5

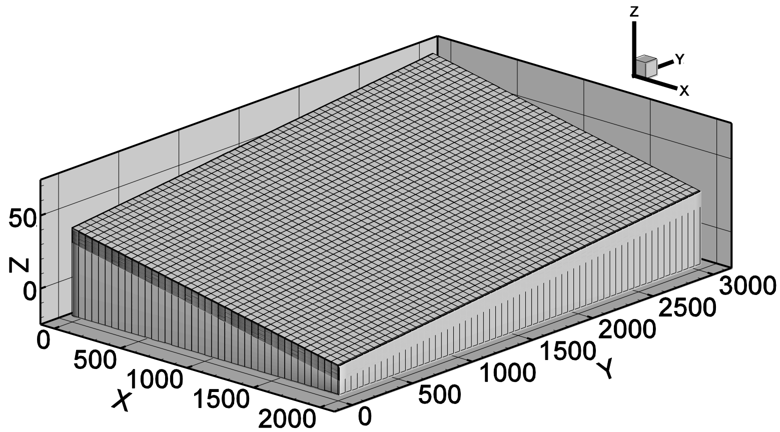

Catchment model for case study (modified version of the V-catchment in Pandy and Huyakorn (2004))

Figure(s)

Figure 6

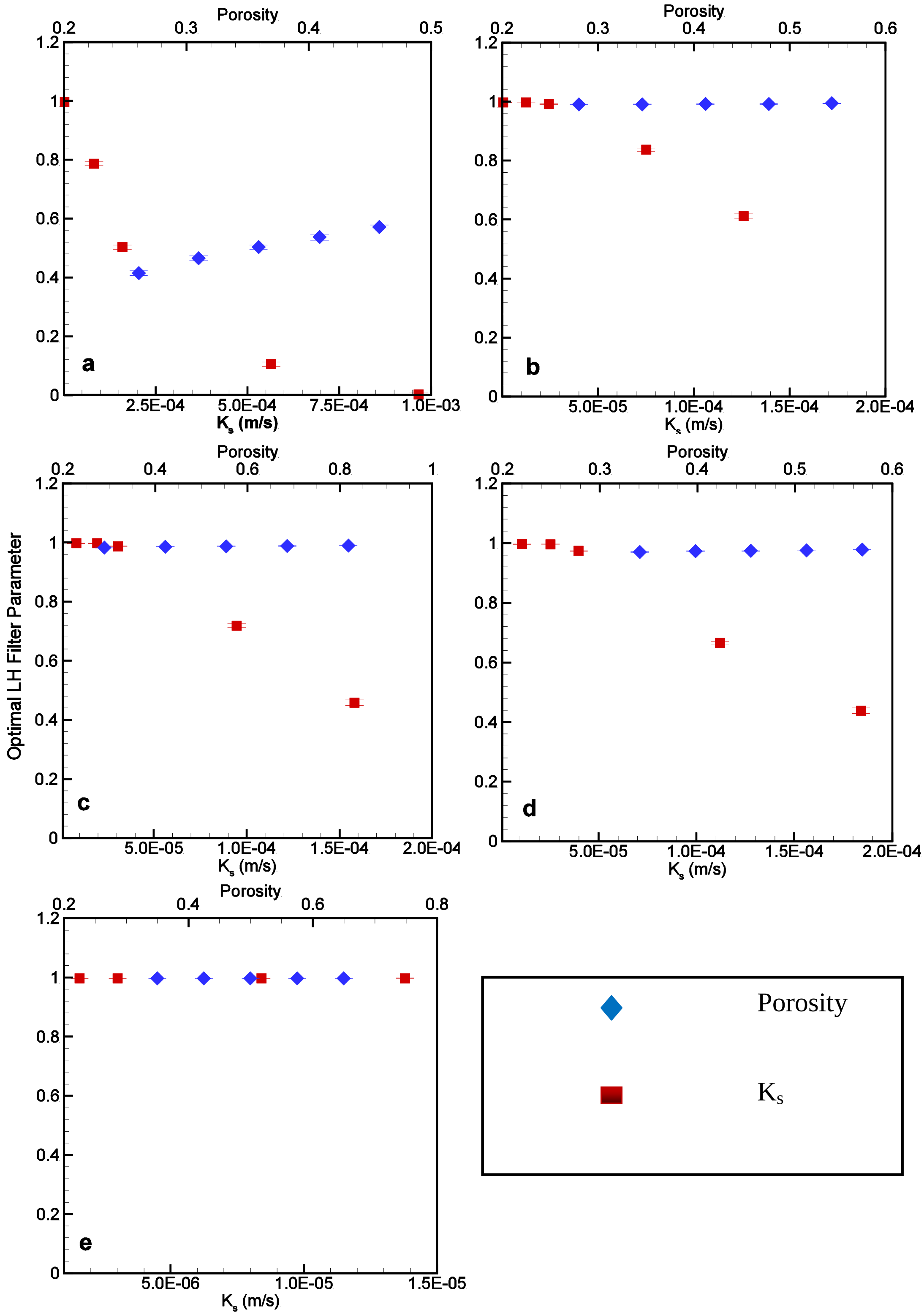

Values of the optimal LH filter parameter with the error bars obtained from the linear estimates of uncertainty for sand (a), sandy loam (b), loam(c), loamy sand (d) and silt loam (e) with different soil properties

Figure 7

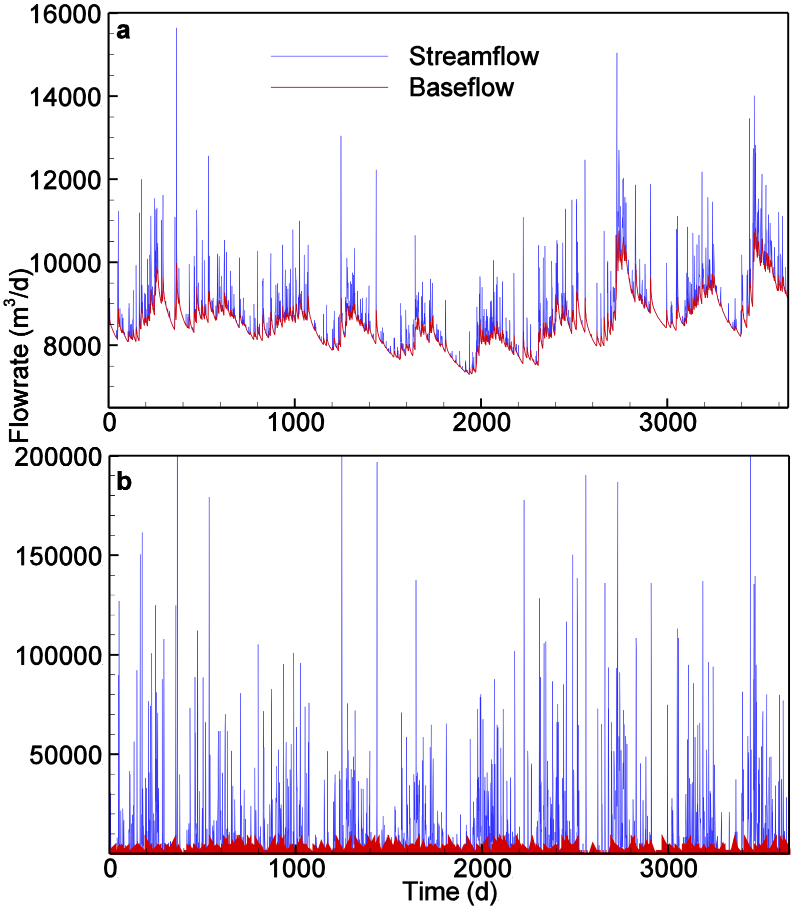

Simulated streamflow and baseflow for catchments with sand (a) and silt loam (b) with their mean values of K_s and porosity

Figure(s)

Figure 8

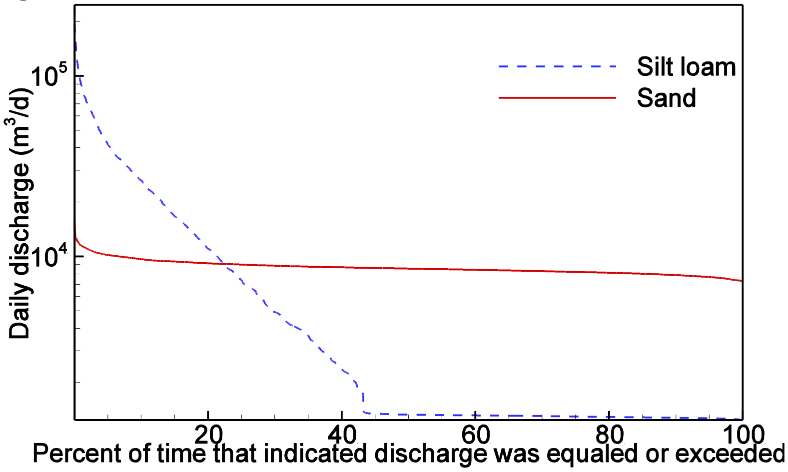

Flow duration curves for catchments with sand and silt loam with their mean values of K_s and porosity

Figure(s)

Figure 9

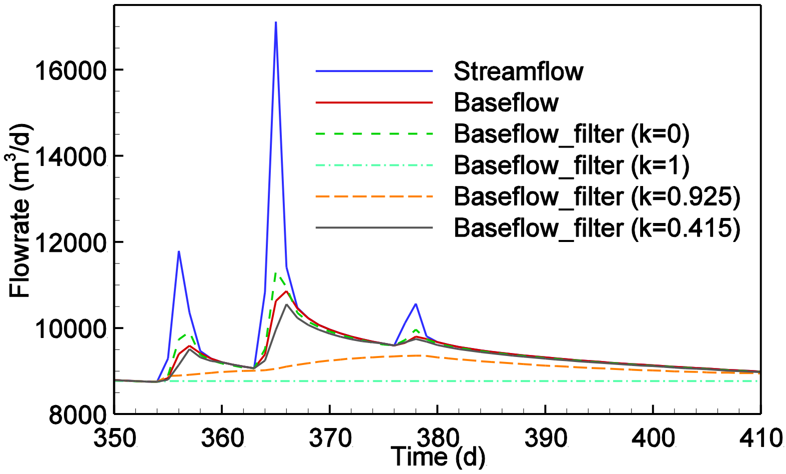

Impact of different values of LH filter parameter on baseflow for catchment with sand with minimum porosity

Figure(s)

Figure 10

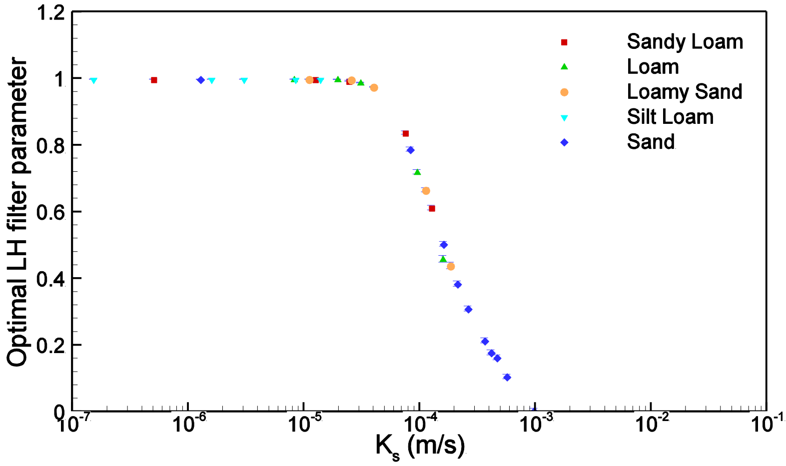

Relationship between the optimal LH filter parameter and K_s with the error bars obtained from the linear estimates of uncertainty for different soil properties

Figure(s)

Figure 11

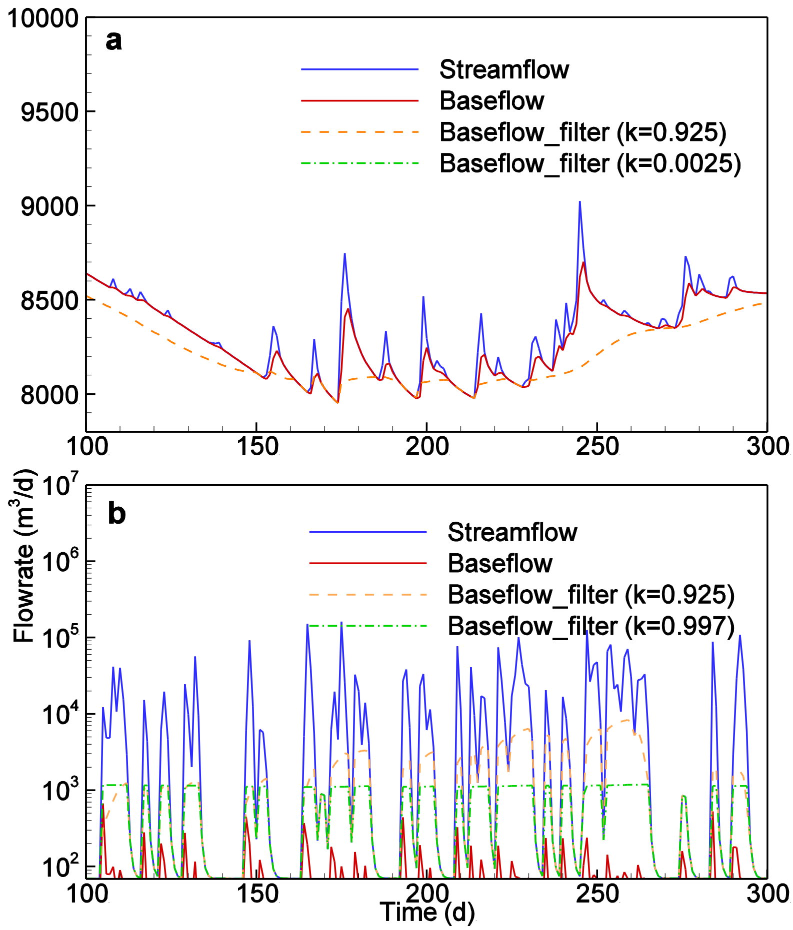

Comparison of baseflow calculated from the HGS model simulation and the LH filter with two different values of the filter parameter for sand with maximum K_s (a) and silt loam with minimum K_s (b)

Figure(s)

Figure 12

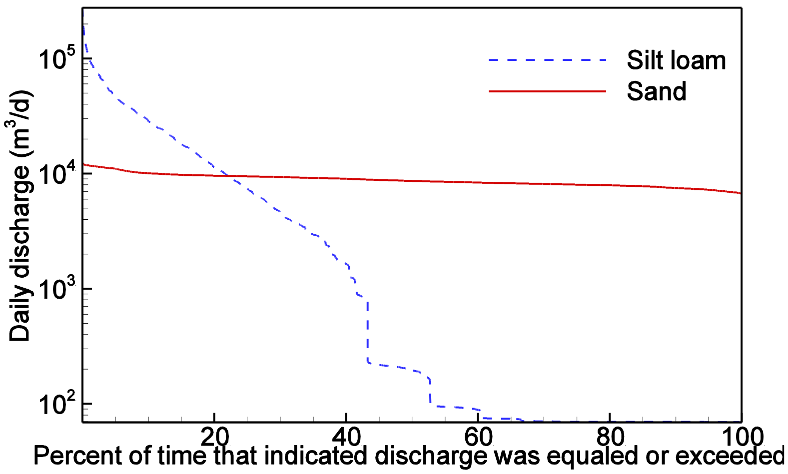

Flow duration curves for catchments with sand with maximum K_s and silt loam with minimum K_s

Table(s)

Table 1 Soil types and ranges and means (shown in brackets) of soil properties considered for model simulations (adopted from Puhlmann et al. (2009))

Soil Type	Porosity	θ_r	K_s (m/s)	α (m^{-1})	N(β)
Sand	0.261-0.4578 (0.359)	0-0.0072 (0.004)	1.27E-6-9.66E-4 (1.6E-4)	0.572-16.412 (8.492)	1.32-8.52 (4.92)
Sandy loam	0.28-0.544 (0.412)	0-0.22 (0.108)	5.01E-7-1.26E-4 (2.44E-5)	0.47-11.75 (6.11)	1.2-5.16 (3.18)
Loam	0.29-0.818 (0.554)	0-0.456 (0.228)	6.31E-7-1.58E-4 (3.07E-5)	0.68-14.56 (7.418)	1.0822-2.252 (1.682)
Loamy sand	0.341-0.569 (0.455)	0-0.1584 (0.079)	1.42E-6-1.84E-4 (3.99E-5)	0.544-17.344 (8.944)	1.2821-2.2661 (1.774)
Silt loam	0.35-0.65 (0.5)	0-0.3 (0.15)	1.51E-7-1.38E-5 (3.01E-6)	0.18-10.98 (5.58)	1.15-3.55 (2.35)

Table(s)

Table2. Optimal LH filter parameters and the linear estimates of uncertainty for sand, sandy loam, loam, loamy sand and silt loam with different soil properties

Soil Type	Min~Max	K_s & related optimal LH filter parameter				Porosity & related optimal LH filter parameter			
		K_s (m/s)	Filter Parameter	Lower Bound	Upper Bound	Porosity	Filter Parameter	Lower Bound	Upper Bound
Sand	Min	1.27E-06	0.997	0.9969	0.9976	0.261	0.415	0.4077	0.4241
	Lower Quartile	8.26E-05	0.787	0.7821	0.7937	0.31	0.465	0.458	0.4733
	Mean	1.60E-04	0.503	0.4956	0.5104	0.359	0.503	0.4956	0.5104
	Upper Quartile	5.65E-04	0.105	0.098	0.1142	0.409	0.537	0.5293	0.5474
	Max	9.66E-04	0.0021	0.0	0.01	0.4578	0.571	0.5635	0.5777
Sandy Loam	Min	5.01E-07	0.997	0.9969	0.9975	0.28	0.990	0.989	0.9907
	Lower Quartile	1.25E-05	0.997	0.9967	0.9982	0.346	0.991	0.9898	0.9916
	Mean	2.44E-05	0.992	0.9914	0.9938	0.412	0.992	0.9914	0.9938
	Upper Quartile	7.51E-05	0.837	0.833	0.8427	0.478	0.992	0.9913	0.9934
	Max	1.26E-04	0.612	0.605	0.6186	0.544	0.994	0.9929	0.995
Loam	Min	8.17E-06	0.997	0.9967	0.9978	0.29	0.983	0.9815	0.9836
	Lower Quartile	1.57E-05	0.997	0.9963	0.9979	0.422	0.986	0.9846	0.9864
	Mean	3.07E-05	0.987	0.9864	0.988	0.554	0.987	0.9864	0.988
	Upper Quartile	9.46E-05	0.719	0.7133	0.7257	0.686	0.988	0.9873	0.9891
	Max	1.58E-04	0.458	0.4501	0.4679	0.818	0.990	0.9885	0.9906
Loamy Sand	Min	1.10E-05	0.997	0.9966	0.9978	0.341	0.970	0.969	0.9713
	Lower Quartile	2.55E-05	0.996	0.9948	0.9967	0.398	0.973	0.9715	0.9738
	Mean	3.99E-05	0.974	0.9732	0.9753	0.455	0.974	0.9732	0.9753
	Upper Quartile	1.12E-04	0.665	0.6582	0.6713	0.512	0.976	0.975	0.9769
	Max	1.84E-04	0.438	0.4304	0.4477	0.569	0.978	0.9772	0.9794
Silt Loam	Min	1.51E-07	0.997	0.9968	0.9974	0.35	0.997	0.9968	0.9977
	Lower Quartile	1.58E-06	0.997	0.9969	0.9976	0.425	0.997	0.9968	0.9977
	Mean	3.01E-06	0.997	0.9968	0.9977	0.5	0.997	0.9968	0.9977
	Upper Quartile	8.41E-06	0.997	0.9967	0.9979	0.575	0.997	0.9968	0.9977
	Max	1.38E-05	0.997	0.9967	0.9982	0.65	0.997	0.997	0.9973

Table(s)

Table3. Comparison of LH filter performance for the case where the optimal filter parameter was used and a filter parameter of 0.925 was used for sand, sandy loam, loam, loamy sand and silt loam with different K_s

Soil type	K_s (m/s)		E_f between simulated baseflow and that obtained using LH filter with the optimal filter parameter	E_f between simulated baseflow and that obtained using LH filter with a filter parameter of 0.925
Sand	Min	1.27E-06	-2.266	-19.613
	Lower quartile	8.26E-05	0.960	0.900
	Mean	1.60E-04	0.989	0.903
	Upper quartile	5.65E-04	0.999	0.969
	Max	9.66E-04	0.9998	0.976
Sandy loam	Min	5.01E-07	-10.29	-73.56
	Lower quartile	1.25E-05	-0.044	-1.945
	Mean	2.44E-05	0.290	-0.679
	Upper quartile	7.51E-05	0.965	0.946
	Max	1.26E-04	0.981	0.900
Loam	Min	8.17E-06	-0.135	-2.704
	Lower quartile	1.57E-05	0.010	-1.613
	Mean	3.07E-05	0.517	-0.078
	Upper quartile	9.46E-05	0.958	0.888
	Max	1.58E-04	0.986	0.884
Loamy sand	Min	1.10E-05	-0.083	-2.136
	Lower quartile	2.55E-05	0.137	-1.125
	Mean	3.99E-05	0.825	0.698
	Upper quartile	1.12E-04	0.981	0.924
	Max	1.84E-04	0.991	0.906
Silt loam	Min	1.51E-07	-76.85	-489.41
	Lower quartile	1.58E-06	-1.603	-14.84
	Mean	3.01E-06	-0.589	-6.966
	Upper quartile	8.41E-06	-0.130	-2.651
	Max	1.38E-05	-0.029	-1.813